An Acad Bras Cienc (2025) 97(4): e20250053 DOI 10.1590/0001-3765202520250053
Anais da Academia Brasileira de Ciências | *Annals of the Brazilian Academy of Sciences*
Printed ISSN 0001-3765 I Online ISSN 1678-2690
www.scielo.br/aabc | www.fb.com/aabcjournal

CHEMICAL SCIENCES

Recycling and reuse of polyurethane mattresses for recovering oils spilled in seawater

KESLEI ROSENDO DA ROCHA, OSVALDO CHIAVONE-FILHO & HUMBERTO NEVES MAIA DE OLIVEIRA

Abstract: In this work, polyurethane foams from post-consumer mattresses were recycled through surface modifications and reused to recover oils spilled in seawater. The surface modifications included grafting zinc oxide followed by coating with hexadecanoic acid, which enhanced the foams' hydrophobicity and oil affinity. Sorption tests simulating oil spills were conducted on three systems involving seawater and oil (diesel, S46 lubricating, or 20W40 engine). The modifications led to increased oil sorption capacity, achieving up to 950% in the seawater-20W40 engine oil system. Additionally, the modification reduced the seawater sorption by up to 72% in the seawater-diesel system. The findings indicated that viscosity significantly affects mass transport between the adsorbate and adsorbent. Verhuls' kinetic model was the best fit for the sorption of diesel, S46 lubricating, and 20W40 engine oil ($R^2 = 0.99$). The pseudo-second-order model was also suitable for diesel and S46 lubricating oil ($R^2 > 0.98$). The desorption kinetics and reuse tests demonstrated that the foams effectively retained over 83% of absorbed oil after 30 minutes in suspension and maintained this capacity for over 50 cycles. This study highlights the successful application of one residue as an effective agent for the removal of another, demonstrating its potential for sustainable remediation strategies.

Key words: Oil spill, Reuse of polymers, Solid waste management, Surface modification.

INTRODUCTION

Coal and petroleum are currently the world's primary energy sources, and their importance for maintaining global society is undeniable (Gyamfi et al. 2021, Wang 2023). Brazil does not depend on coal, but petroleum and other liquid fuels have been responsible for supplying nearly 46% of Brazil's domestic energy usage (Wang 2023), which shows how vital petroleum exploration still is.

Petroleum can be obtained on continents and islands (onshore) as well as underneath the oceans (offshore). As in any industrial activity, petroleum exploration is not free of potential accidents. During well drilling, extraction, and transportation, accidental spills may occur and cause severe environmental impacts (Hamacher et al. 2022, Inojosa et al. 2022, Miranda et al. 2022, Nobre et al. 2022). When they occur, the first step is to contain the spilled oil to prevent it from spreading and then remove it by applying the most appropriate technique (Abernathy et al. 1989).

Currently, incineration, pumping, and chemical dispersants are some of the methods used to remove oil spilled at sea (Abernathy et al. 1989, Dave & Ghaly 2011). Incineration produces toxic gases that the action of the winds can quickly spread, putting technical teams working at the accident site and entire cities nearby at risk (Li et al. 2020). Pumping

employing skimmers, for example, may present a loss of efficiency in the case of rough seas, in addition to being clogged in the event of debris and ice (Li et al. 2016). Chemical dispersants reduce this problem, but they might not be the most suitable solution, especially in the case of highly viscous oils and at low temperatures (Silva et al. 2022). To address the limitations of traditional methods, alternatives, such as sorption in porous polymeric structures, have been developed to recover spilled oils (Li et al. 2012, Costa et al. 2017, Ko et al. 2020).

Polyurethane flexible foams are highly porous polymers capable of absorbing fluids (Li et al. 2012). However, they are poorly selective and simultaneously absorb water and oil in high quantities. The main application of polyurethane flexible foam is for upholstery and mattress production (Grotto et al. 2020). After the end of its commercial life, foams must be appropriately disposed of following proper environmental guidelines. Unfortunately, it is common to find post-consumer polyurethane mattresses discarded in landfills or vacant lots throughout cities. In the European Union alone, approximately 30 million mattresses are turned into garbage annually, where 60% of this waste ends up in landfills, and the remainder is incinerated (Veses et al. 2021). Brazil faces a similar problem: mattresses being discarded irregularly throughout major Brazilian cities and high volumes of foam occupying landfills (Moura et al. 2022). Since 2014, Brazil has produced more than 1,000,000 m^3 of new polyurethane foam each day, increasing the need for studies on its recycling and reuse after its commercial life (Grotto et al. 2020).

Although polyurethane foams are not very selective, changing this behavior through surface modifications that enable greater selectivity for oils over water is possible. Post-consumer foam modification must be simple and inexpensive to be viable. Research on new polyurethane foam coatings can be found in the literature (Li et al. 2012, Ko et al. 2020, Zhang et al. 2022, Wu et al. 2023). However, no reports were found about the use of post-consumer foams for oil recovery, highlighting the originality and innovation of this work.

Recycling and reusing foams from polyurethane mattresses is an effective way to reduce solid waste in cities worldwide. This work is innovative, as it establishes, in an unprecedented manner, a practical application of the 3Rs - reduce, reuse, and recycle - in the context of post-consumer mattress foams to recover oil spills. The techniques presented here for recycling post-consumer foam through surface modifications and reusing it as an oil adsorbent has the potential to yield results that are comparable to or even superior to those achieved with newly synthesized foams. This initiative enables the use of one type of waste to help remove another, promoting economic circularity and minimizing the environmental impact of the petrochemical industry.

MATERIALS AND METHODS

Materials

Post-consumer (PC) polyurethane foam was recovered from an irregular disposal area beside a highway. The label on the mattress registered a density of 23 $g{\cdot}L^{-1}$. Although dirty, there were no signs of physical damage or visible compaction. The foam was washed with 70% ethanol and oven-dried at 60 °C to a constant mass. It was then cut into 1 cm x 1 cm x 1 cm cubes for modification, characterization, and testing. All reagents used in this work were purchased from Synth, Brazil, and used as received. Diesel and 20W40 engine oil were obtained from Distribuidora BR, Brazil. S46 lubricating oil was obtained from Montreal, Brazil. Seawater was obtained from the coast of

Natal, RN (5°52'04.7"S 35°10'40.9"W) and filtered through blue band filter paper to remove sand and other solid debris.

Surface modification

Grafting with zinc oxide (ZnO) rods was performed in two stages, adapting the methodology of Li et al. (2015) and Rocha et al. (2023a).

In the first stage, a 1 $mol \cdot L^{-1}$ potassium hydroxide solution was added dropwise to a 1×10^{-1} $mol \cdot L^{-1}$ zinc acetate dihydrate solution until the pH reached 11. Both solutions included methanol as a solvent. The mixture was mechanically stirred at 510 rpm for 90 min and then centrifuged at 3500 rpm for 10 min. The supernatant was discarded, and the precipitate was resuspended in distilled water. The foam cubes were submerged for 5 min in the suspension and then cured in a vacuum oven at 170 °C for 12 min. The soaking and curing procedures were repeated three times.

In the second stage, the foams from the first stage were submerged in a 3×10^{-3} $mol \cdot L^{1}$ zinc nitrate hexahydrate and 3×10^{-3} $mol \cdot L^{-1}$ hexamethylenetetramine mixture. The mixture and the foams were kept in a water bath for 180 min at 90 °C. Finally, the foams were compressed and dried in an oven at 60 °C.

The foams grafted with ZnO were immersed for 48 h in a 1×10^{-2} $mol \cdot L^{-1}$ hexadecanoic acid (HA) solution using anhydrous ethanol as the solvent. The cubes were subsequently dried in an oven at 60 °C, resulting in a foam labeled as ZnO/HA-PC.

Characterizations

The foams before and after modifications were characterized by scanning electron microscopy (SEM) + energy dispersion X-ray spectroscopy (EDS) (Jeol, JSM - 6610LV, Japan), X-ray diffraction (XRD) (Bruker, D8 Advance, USA), Fourier transform infrared spectroscopy (FTIR) (Shimadzu, Iraffinity-1, Japan), and contact angle measurements via goniometer (Kruss, DSA 100, Germany).

The mean pore diameter of the foams was determined through SEM images via free ImageJ software. The volume, bulk density, and average porosity were calculated according to the literature (Wu et al. 2019). The seawater used in the tests was characterized by temperature, pH, turbidity, conductivity, salinity, and density. The oils used in the tests were characterized in terms of temperature, viscosity, and density.

Sorption capacity in water-oil system

The sorption tests were conducted following the ASTM F726/D95 methodology (ASTM 2017, 2023). In a wide-mouth Erlenmeyer flask, a suspension composed of 92% seawater and 8% oil was prepared with enough volume to ensure that the foam cubes remained fully immersed during the test. One foam cube was added to each flask, and the mixture was stirred at 150 rpm using a Kline-type stirrer. The oils tested included diesel, S46 lubricating oil, and 20W40 engine oil.

After 15 minutes of stirring, the agitation was halted, and each foam cube was carefully and individually transferred to a round-bottom distillation flask. Distillation was performed using a borosilicate distillation unit equipped with a Dean Stark apparatus (ASTM D95) and turpentine as the solvent. The distillation process was deemed complete when the meniscus on the graduated scale of the Dean Stark apparatus did not change for more than one minute.

The volume of seawater recorded on the graduated scale allowed for the determination of the seawater and oil content sorbed by each foam cube. One-way analysis of variance was employed to assess statistical significance via Statistica 7 software.

Sorption kinetics in water-oil system

Several mathematical models were used to analyze the sorption behavior of seawater and oils in water-oil systems. Model fitting and parameter calculations were performed using Origin 2016 software. All the data were collected at 23 °C ± 1 °C.

The following kinetics models were employed to fit the experimental data: Equation 1 is the Lagergren model (Lagergren 1898), Equation 2 is the model by Ho & McKay (1999), Equation 3 represents the Elovich model (Roginsky & Zeldovich 1934), Equation 4 is the Weber & Morris (1963) model, and Equation 5 is the Verhulst model (Bacaër 2011), as compiled in Table I. To assess the suitability of each model in fitting the experimental data, the coefficient of determination (R^2) and the sum of squared residuals (SSR) were calculated.

Retention-dripping kinetics

The experiment was conducted in a single-component oil system, where diesel, S46 lubricating oil, and 20W40 engine oil were tested. Following ASTM F726 (ASTM 2017) and adaptations made by Cojocaru et al. (2011), glass beakers were filled with enough oil to ensure that the foams remained submerged. One foam cube was placed in each beaker, and the foams were allowed to remain in contact with the oil for 15 minutes. Preliminary tests showed that the volume of oil absorbed did not change after this period. After 15 minutes, each foam cube was removed from the beaker using a mesh basket with 0,2 cm openings, which was suspended over a calibrated analytical balance (as illustrated in Figure 6). The balance had been tared to account for the weight of the mesh basket. The weight of the desorbed oil droplets

Table I. Kinetic models and their parameters applied to fit experimental sorption data.

Kinetic Model	Sorption rate	Sorption capacity	Parameters
Equation 1 Pseudo-First Order (Lagergren)	$\frac{dq_t}{dt} = k_1 \cdot (q_e - q_t)$	$q_t = q_e \cdot (1 - e^{-k_1 \cdot t})$	k_1 ($g \cdot g^{-1} \cdot s^{-1}$) Qe ($g \cdot g^{-1}$)
Equation 2 Pseudo-Second Order (Ho & McKay)	$\frac{dq_t}{dt} = k_2 \cdot (q_e - q_t)^2$	$q_t = \frac{k_2 \cdot q_e^2 \cdot t}{1 + k_2 \cdot q_e \cdot t}$	k_2 ($g \cdot g^{-1} \cdot s^{-1}$) Qe ($g \cdot g^{-1}$)
Equation 3 Chemisorption (Elovich)	$\frac{dq_t}{dt} = \alpha \cdot e^{-\beta q_t}$	$q_t = \frac{1}{\beta} \cdot \ln(1 + \alpha \cdot \beta \cdot t)$	α ($g \cdot g^{-1} \cdot s^{-1}$) β ($g \cdot g^{-1}$)
Equation 4 Intraparticle diffusion (Weber & Morris)	-	$q_t = K_d \cdot t^{0,5} + C$	k_d ($g \cdot g^{-1} \cdot s^{-0.5}$) C ($g \cdot g^{-1}$)
Equation 5 Logistic (Verhulst)	$\frac{dq}{dt} = c \cdot q \cdot (1 - \frac{q}{a})$	$q_t = \frac{a}{1 + b \cdot e^{-c \cdot t}}$	a ($g \cdot g^{-1}$); b c (s^{1})

q_t ($g \cdot g^{-1}$) is the amount of fluid sorbed at any time t (s); q_e ($g \cdot g^{-1}$) is the amount of fluid sorbed at equilibrium (after a long period of exposure to the adsorbate); k_1 ($g \cdot g^{-1} \cdot s^{-1}$), k_2 ($g \cdot g^{-1} \cdot s^{-1}$), k_d ($g \cdot g^{-1} \cdot s^{-0,5}$), α ($g \cdot g^{-1} \cdot s^{-1}$), and c ($s^{-1}$) are kinetic constants of their respective models and are responsible for the angular coefficient (slope) of the kinetic curves; β ($g \cdot g^{-1}$), C ($g \cdot g^{-1}$), a ($g \cdot g^{-1}$), and b (dimensionless) are constants of their respective models.

was tracked throughout the test period as they dripped from the foams. All experimental data were collected in triplicate at a temperature of 23 °C ± 1 °C.

Bazargan et al. (2015b) conducted complementary studies to the ASTM F726 standard (ASTM 2017) to minimize inconsistencies and contribute to the standardization of reports on oil sorption studies. In their most comprehensive study, Bazargan et al. (2015a) developed, analyzed, and validated a model for unstable retention states regarding fluid desorption from sorbents. Equation 6 (unnormalized) and Equation 7 (normalized) are outcomes of the work of Bazargan et al. (2015a) and can estimate the desorption of fluids that have been sorbed by the saturated adsorbent. Equation 8 presents the calculation for normalized retention.

$$U_t = U_L e^{-kt} + U_e \quad (6)$$

$$R_L = R_L e^{-kt} + R_e \quad (7)$$

$$R_t = \frac{U_t}{U_{ta}} \quad (8)$$

Where U_t ($g \cdot g^{-1}$) is the uptake capacity of the foam at any time t (s); U_L ($g \cdot g^{-1}$) is the uptake capacity lost due to dripping; U_e ($g \cdot g^{-1}$) is the equilibrium uptake capacity obtained after a long dripping period; k (s^{-1}) is a parameter (Kamaan coefficient) that controls the curvature of the uptake profile; R_t is the normalized retention at any time t (s); R_L is the normalized uptake loss; R_e is the normalized equilibrium uptake capacity obtained after a long dripping period; U_{ta} is the sorption capacity recorded at the first moment.

The experimental data on retention (and dripping loss) of the fluids sorbed in the foams were modeled using Equations 6-8 through nonlinear regression. Model fitting and parameter calculations were performed using Origin 2016 software.

Oil desorption and foam reuse

To assess the reusability of the modified foam in continuous sorption and desorption cycles, the ZnO/HA-PC foam was tested in multicomponent seawater-oil systems, including diesel, S46 lubricating oil, and 20W40 engine oil, following the ASTM F726 standard (ASTM 2017).

In a wide-mouth Erlenmeyer flask, a suspension composed of 92% seawater and 8% oil was prepared with enough volume to ensure that the foam cubes remained fully immersed during the test. One foam cube was added to each flask, and the mixture was stirred at 150 rpm using a Kline-type stirrer. After 15 minutes, stirring was stopped, and the foam cubes were transferred to a vise to be compressed, allowing the seawater and oil to be desorbed (as shown in Figure 7). The same clamping force was applied for all tests, and loosening occurred once there was no longer any visible dripping. The desorbed foam cubes were then placed back into new Erlenmeyer flasks containing the same suspension composition as in the initial test. This process of sorption and desorption was repeated 50 times, and all tests were conducted in triplicate. A one-way analysis of variance was performed to assess statistical significance using Statistica 7 software.

RESULTS AND DISCUSSION

Modifications

The graft allowed the ZnO rods to interact with the polyurethane structure. Hydrogen bonds are formed between the polyurethane and the ZnO during rod growth, as shown in Figure 1a. The connection between ZnO and hydrogen reduces the strength of the hydrogen bond between H-N (hydrogen-nitrogen) in polyurethane. A powerful polar bond forms when hydrogen is chemically connected with fluorine, oxygen, and nitrogen (Grabowski 2020). Since the modification goal

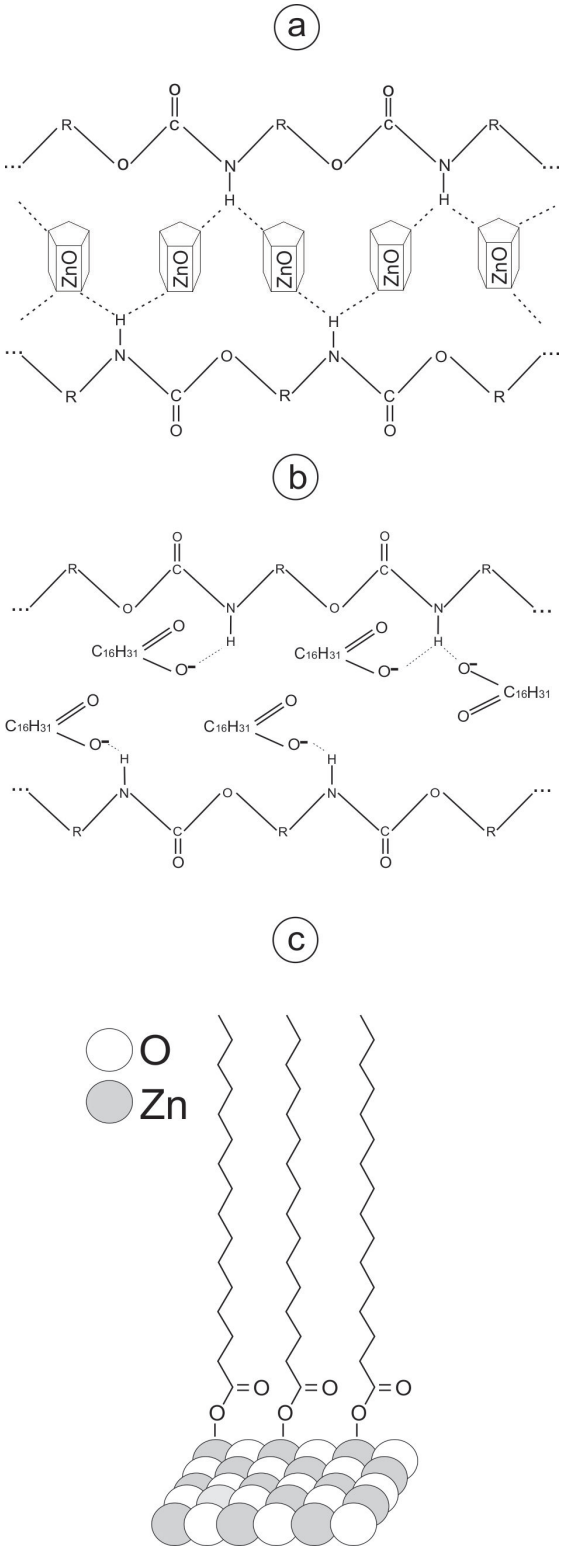

Figure 1. Illustration of steps for post-consumer polyurethane modification: ZnO grafting (a), coating with HA (b), and ZnO grafting followed by coating with HA (c).

is to reduce the polarity of polyurethane foam, decreasing the H-N strength is essential. Dorraji et al. (2018) and Rahman (2020) also associated the preference for ZnO to bond with the N-H groups in different polyurethanes, either during the synthesis process or as a graft.

During coating modification, interactions between HA and polyurethane are controlled by dipole-induced forces (Figure 1b). Coating polyurethane has the potential to increase interaction with the oils during sorption.

The modification order might influence the sorption efficiency. As the graft with ZnO occurs first, followed by the coating with HA, the second interacts preferentially with the first (Figure 1c). Segovia et al. (2011) studied the ability of ZnO to form sheets with organic compounds, especially with carboxylic acids. There is believed to be an induced dipole attraction between the carboxyl radical of organic acids and the metallic part of inorganic structures. The same observation was made by Trino et al. (2018), who identified the preference of groups with greater intermolecular strength in organic molecules (carboxyl) for interactions with ZnO.

In the presence of water, including humidity, zinc oxide (ZnO) exhibits hydrophilic properties due to the interaction between electrons from the oxide (O^{2-}) and the hydroxyl group (OH^-) present in water. However, this hydrophilic affinity can be influenced by the geometry of the oxide (Li et al. 1999, Ennaceri et al. 2016). Different synthesis methods for ZnO lead to variations in geometry, which in turn affect its properties, including hydrophilicity and hydrophobicity (Myint et al. 2013, Ennaceri et al. 2016).

Myint et al. (2013) explain that a material's wettability is directly related to its morphology and the surface energy required to interact with fluid substances. They also note that the surface roughness of the oxide structure could be crucial in determining its behavior, shifting from

hydrophilic (where the contact angle between a water droplet and the surface is less than 90°) to hydrophobic (where the contact angle is greater than 90°).

The impact of surface roughness on the affinity or repulsion of water on solid surfaces was first explored by Wenzel (1936) and later by Cassie & Baxter (1944). Wenzel (1936) developed equations to explain that hydrophilicity occurs when the adsorbate provides a high effective surface area. In this scenario, water droplets tend to maintain complete contact with the surface; thus, smoother surfaces exhibit greater contact area and enhanced hydrophilicity (Wenzel 1936).

Conversely, Cassie & Baxter (1944) noted that increased surface roughness makes it more difficult for water droplets to contact the adsorbate surface due to its irregularities. Additionally, air bubbles can become trapped between the water droplets and the textured surface, reducing adhesion and interaction (Cassie & Baxter 1944). In conclusion, both the findings of Wenzel (1936) and Cassie & Baxter (1944) indicate that a decrease in the effective surface area of the adsorbate in contact with water droplets leads to increased hydrophobicity.

Combining the findings of Wenzel (1936) and Cassie & Baxter (1944) with those of Myint et al. (2013), who studied the behavior of materials transitioning between hydrophilic and hydrophobic states, Ennaceri et al. (2016) provided studies on the hydrophobicization of ZnO by adjusting its geometry during the synthesis process. By combining the roughness and geometry of ZnO, it is possible to reduce its wettability and enhance its preference for oily substances.

Li et al. (2015) synthesized ZnO by combining sol-gel and hydrothermal methods adjusting reaction parameters to produce microrods made up of rough multilayers of the oxide using polyurethane foams as support. To enhance the hydrophobic properties of the ZnO microrods, they coated them with HA. The bond between the oxide and the fatty acid, which increases hydrophobicity, was studied in detail by Segovia et al. (2011) and Trino et al. (2018). Additionally, Agrawal et al. (2017) focused on the synthesis of ZnO and its coating with HA to improve hydrophobicity on adsorbate surfaces.

Li et al. (2015) investigated the hydrophobization mechanism through the joint modification of ZnO and HA on new polyurethane surfaces. In contrast, Rocha et al. (2023a) examined the hydrophobization mechanism on the same type of surface but focused on the separate application of ZnO and HA. The foams modified only with HA exhibited poor oil sorption results. In contrast, the foams modified with ZnO achieved sorption capacities of up to 44 $g \cdot g^{-1}$, maintaining reusability for at least 10 sorption/desorption cycles (Rocha et al. 2023a). Similarly, the findings of Li et al. (2015) regarding the ZnO/HA combination for oils akin to those tested by Rocha et al. (2023a) also reached a sorption capacity of 44 $g \cdot g^{-1}$, but showed reusability with minimal losses over more than 50 sorption/desorption cycles.

In terms of oil sorption, the results of Rocha et al. (2023a), which involved modifying polyurethane solely with ZnO, were similar to those of Li et al. (2015), who combined ZnO rods with HA. However, the two studies differed in their reuse capacity. Therefore, the combined modification was selected for further investigation in this present work.

Characterizations

The unaltered post-consumer foams (Un-PC) presented a smooth pore surface (Figure 2b). In contrast, foams modified with a combination of grafting and coating (ZnO/HA-PC) developed roughness (Figure 2d). Figure 2d highlights the formation of ZnO sheets coated with HA. EDS

(Figure 2a and Figure 2c) revealed the presence of carbon, nitrogen, and oxygen in both foams (as expected since these are fundamental elements of the polyurethane polymer). Zinc, as expected, was identified only in the foam grafted with this element (Figure 2c). Although calcium is not part of the original polymer composition, it was identified in both foams due to its addition as a "filler" in the expansion process (Sant'anna et al. 2008).

The mean pore diameters of the Un-PC and ZnO/HA-PC foams were 252.676 ± 89.814 µm and 369.026 ± 93.626 µm, respectively (100 pores were measured for each). The increase in average size can be explained by the modification process to which the foam was subjected. The growth steps for ZnO rods include prolonged heating with hot solvent submersion, which can result in pore expansion. With the solidification of the rod, it is possible that the pores remained permanently dilated.

Maia et al. (2024) synthesized castor oil-based polyurethane foam incorporating macadamia nutshell waste for the purpose of oil spill recovery. The average pore size of the unmodified castor oil-based polyurethane foam was 276 ± 82 µm, which is similar to the average pore size observed in the Un-PC foam. In contrast to the findings for ZnO/HA-PC, the foams modified with macadamia nutshell waste exhibited a decrease in average pore size as the amount of waste incorporated increased. This reduction can be attributed to the fact that the macadamia nutshell waste was integrated during the synthesis process, becoming part of the original structure, with the expansion limited

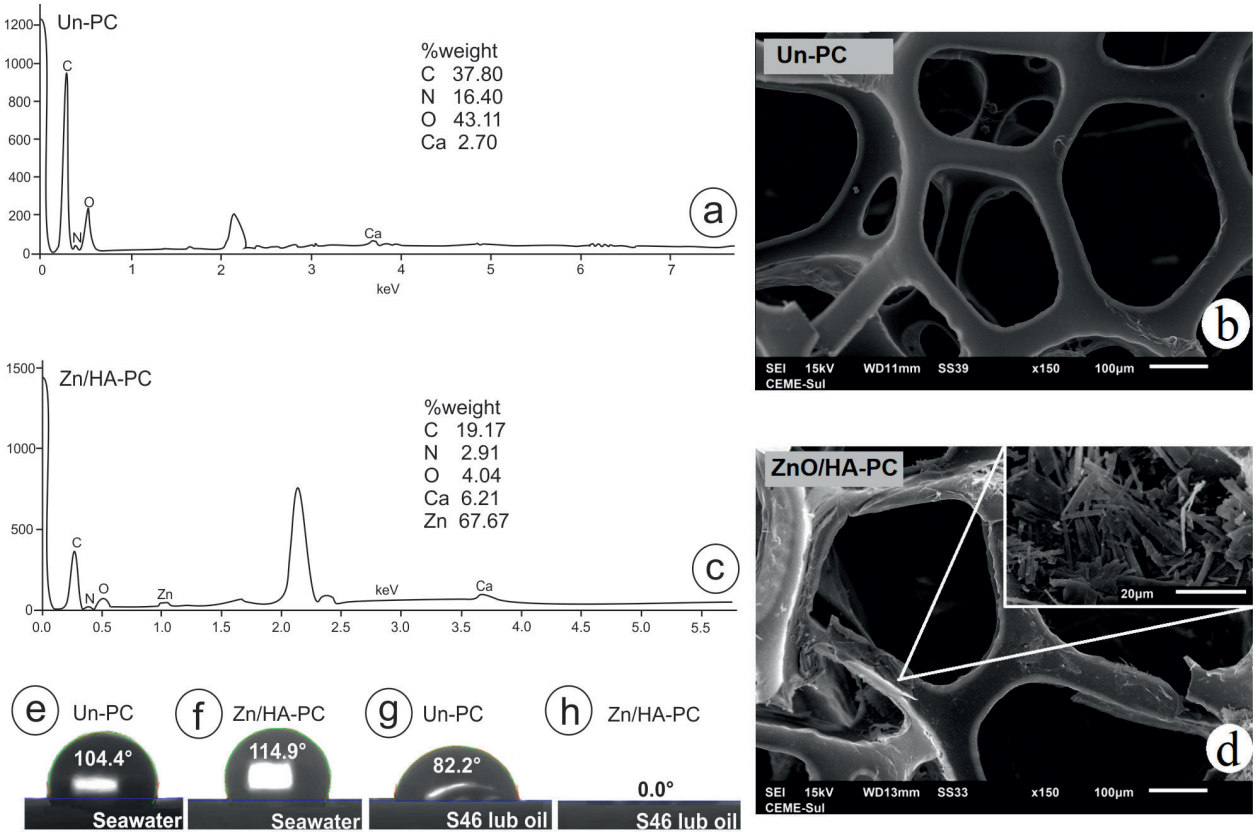

Figure 2. EDS, SEM, and contact angle before (a, b, e, and g, respectively) and after (c, d, f, and h, respectively) ZnO grafting + HA coating.

by the fixed volume of the mold. Consequently, as the waste content increased within the same volume, the expansion led to a compression of the pores, resulting in the smaller average pore size reported by Maia et al. (2024).

The greater the contact angle between the water droplet and the surface under analysis, the more hydrophobic the surface is. In contrast, the smaller the contact angle between the oil droplet and the surface, the more oleophilic the surface is. The contact angle between the seawater droplet and the polyurethane surface increased by 10.5° after the combined modification (Figure 2e and Figure 2f). The reduction in the contact angle between the droplet of S46 lubricating oil and the polyurethane surface was greater than 82° for the modified surface (Figure 2g and Figure 2h). Although the increase in hydrophobization was modest, the increase in oil affinity caused by the modifications was very significant.

Maia et al. (2024) synthesized polyurethane foam based on castor oil, incorporating macadamia nutshell waste for the purpose of oil spill recovery. The contact angle measured between a water droplet and the surface of the castor oil-based polyurethane foam was found to be 95.3°. A tendency was observed between the increase in the incorporation of macadamia nutshell waste in the castor oil-based polyurethane foam and the increase in the contact angle between its surface and the water droplet. With 20% (w/w) of incorporated waste (highest value evaluated), the angle reached 119.1°, an increase of almost 24°. In contrast, the modification procedure to obtain the ZnO/HA-PC foam, which fixed only micrograms of ZnO and HA (< 1%), resulted in a hydrophobicity increase of 10.5° - a result that is notably satisfactory when compared to the 20% (w/w) required to achieve the 24° increase observed by Maia et al. (2024).

The synodal curves in the diffractogram (Figure 3) between 10° and 20° for both foams are typical of amorphous structures such as polyurethane (which is an amorphous polymer since it does not have a well-defined spatial order). The peaks observed close to 29° in 2θ correspond to the isocyanate group used in polyurethane synthesis (Zia et al. 2008). The Zn peaks were not identified because the amount grafted onto the foam surface was lower than the detection limit of the employed technique. The behaviors in the diffractograms for polyurethane foam correspond to those reported in the literature (Zia et al. 2008, Wu et al. 2019).

The spectrograms for the Un-PC and ZnO/HA-PC foams were similar (Figure 4). The slight peak near 3338 cm^{-1} is typical for N–H bonds, whereas the peak near 2864 cm^{-1} is characteristic of CH_2 groups. Small peaks at 1713 cm^{-1}, 1528 cm^{-1}, and 1241 cm^{-1} are attributed to the C=O, N-H/C-H, and N-H/C-N bonds, respectively. Finally, the sharpest peak at 1100 cm^{-1} is typical for C-O-C bonds. All those bonds are typical and expected in the polyurethane structure and align with what is observed in the literature (Zia et al. 2008, Caddeo et al. 2014, Pinto et al. 2018).

Although the FTIR spectra for Un-PC and ZnO/HA-PC foams were similar, the peaks in the region near 500 cm^{-1} showed significant differences (Figure 4c). The transmittance decreased in this region for the ZnO/HA-PC foam compared to the Un-PC foam. Oraby et al. (2025) and Zahra et al. (2022) observed a similar phenomenon when comparing the spectra of pure polyurethane with polyurethane modified with ZnO. The decrease occurred in the same region with spectra similar to those shown in Figure 4.

Fakhar et al. (2020) developed membranes from polyurethane foam with different percentages of ZnO. Although the FTIR technique is primarily used for analyzing organic

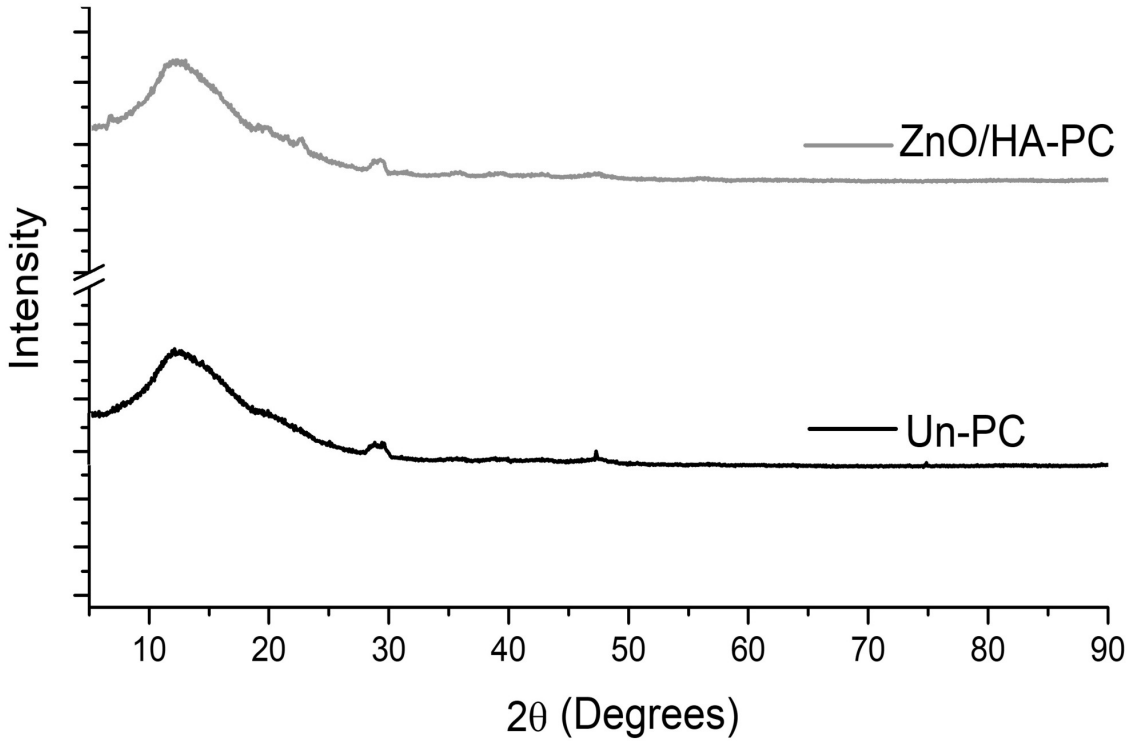

Figure 3. XRD before (Un-PC) and after (ZnO/HA-PC) modifications.

compounds, Fakhar et al. (2020) also employed it to study the ZnO used in the modifications, facilitating comparison between the modified and unmodified foams. The spectrum for pure ZnO was almost linear throughout the test. However, in the 500 cm^{-1} region, an intensely decreasing peak was recorded. As the percentage of ZnO incorporated into the polyurethane foam increased, the intensity of the drop in the 500 cm^{-1} region also became more pronounced. In contrast, no drop was recorded for the unmodified foam.

The findings of Oraby et al. (2025), Zahra et al. (2022), and Fakhar et al. (2020) highlight the influence of ZnO on the structure of polyurethane. However, it can also be concluded that grafting ZnO into polyurethane foams does not lead to significant changes in their organic structure, as shown in Figure 4.

Table II shows that the average volume for the Un-PC foam was slightly lower than that calculated for ZnO/HA-PC (volume = width × length × depth). Both densities were close to those recorded on the commercial label of the post-consumer foam used (23 $g{\cdot}L^{-1}$).

Maamoun et al. (2024) investigated different formulations for synthesizing flexible polyurethane foams and found an antagonistic association between pore size and density: as foam density increases, the average pore size decreases. These findings contrast with those observed between Un-PC and ZnO/HA-PC. However, it is important to note that the association identified by Maamoun et al. (2024) applies to foams with the same volume (more mass over the same volume increases the density and compacts the pores, reducing them).

Prior to modification with ZnO and HA, the post-consumer foam cubes shared similar dimensions and densities. Following the modification, an increase in mass was observed due to the incorporation of ZnO and HA

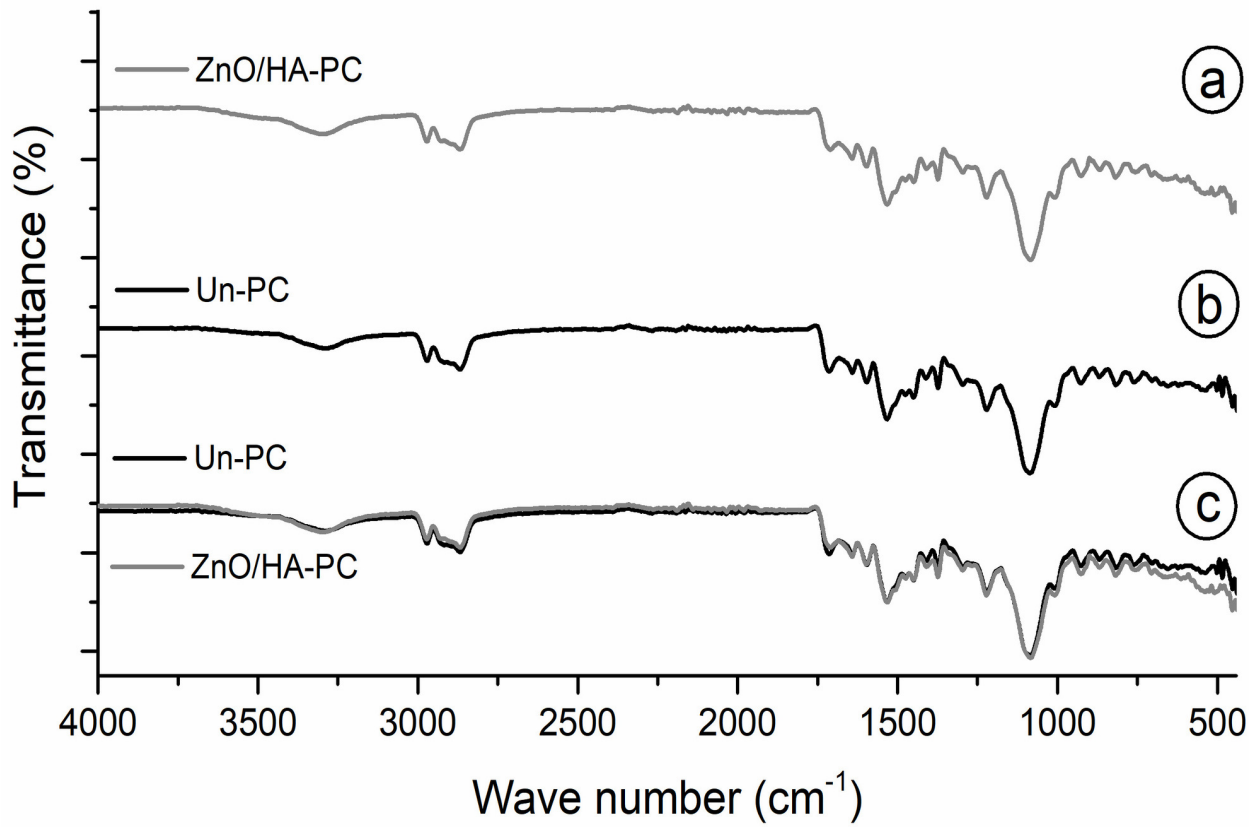

Figure 4. FTIR spectra for ZnO/HA-PC (a) and Un-PC (b) foam presented separately and superimposed (c) to emphasize their differences.

particles, alongside foam expansion resulting from the application of hot solvent. Throughout the curing and drying processes, the modified foam (ZnO/HA-PC) retained a portion of its volumetric expansion due to the solidification of the ZnO rods. This increase in both mass and volume led to a rise in density when compared to the unmodified foam. Additionally, with the volume remaining permanently expanded, the average pore size of the ZnO/HA-PC increased in comparison to the Un-PC.

ZnO/HA-PC had a greater porosity than Un-PC did (Table II). This result agrees with what was observed for the average pore size (determined via ImageJ using the micrographs), where the pores of ZnO/HA-PC (369.026 ± 93.626 µm) were more extensive than those of Un-PC (252.676 ± 89.814 µm). While the average pore size is estimated only in terms of area (two-dimensional), porosity seeks to relate the volume of voids to the total volume of the foam (three-dimensional). The permanent expansion caused by physical-chemical modification with hot solvent increased (+ 25.4%) the average pore size and, consequently, the volume of voids in the modified foam (ZnO/HA-PC). Kardeş et al. (2025) reported an average pore size of approximately 340 ± 50 µm, a porosity of approximately 90%, and a density of 30 $g{\cdot}L^{-1}$ for the polyurethane foam utilized in the immobilization of ZnO nanorods. These findings align with the previously established characteristics for the ZnO/HA-PC foam.

While this work revealed increased porosity after modification (+34.05%), other works reported the opposite results. Wu et al. (2019)

Table II. Volume, density, and porosity of unchanged and modified foams.

	Un-PC	ZnO/HA-PC
Volume (L)	$6.71 \cdot 10^{-3} \pm < 0.001$	$7.31 \cdot 10^{-3} \pm < 0.001$
Density ($g \cdot L^{-1}$)	22.00 ± 0.50	25.00 ± 1.00
Porosity (%)	68.87 ± 11.65	92.32 ± 3.43

reported a 42.81% decrease in porosity between unmodified polyurethane foam and modified with 8% silicone + clay nanotubes. Ng et al. (2020) reported an 8.5% decrease in porosity when comparing polyurethane foam before and after modification with poly perfluorodecyl acrylate.

The properties measured for seawater shown in Table III align with what has been reported in the literature (Silva & Oliveira 2017, Ferreira et al. 2019). The pH of the seawater was slightly alkaline, with elevated salinity and conductivity due to several dissolved salts. The seawater density was slightly greater than 1000 $g \cdot L^{-1}$ because of the extra mass that the dissolved salts added in the measurements.

The kinematic viscosity of all three oils (Table IV) was more significant at room temperature (23 °C) than at 40 °C (as expected since increasing the temperature reduces the viscosity). In all the cases, the oils were less dense than the seawater. The properties determined here align with those reported in the literature (Zaro et al. 2021, Choudhury et al. 2023, Rocha et al. 2023b).

Sorption capacity in water-oil system

Sorption tests were performed on multicomponent systems that simulated oil spills. The results are compiled in Table V. In the first system (8% (v/v) of diesel spilled into seawater), the Un-PC foam showed the highest sorption of diesel and seawater. Compared with the ZnO/HA-PC foam, Un-PC absorbed 261% more seawater and only 20% more diesel. Although the modified foam slightly reduced the sorption capacity of diesel, it strongly reduced the sorption of seawater.

Martins et al. (2021) developed a polyurethane foam reinforced with palm fiber residues and assessed its effectiveness in recovering oil and water in both single-component and multicomponent systems. In the S500 diesel:seawater system (4 g : 0,05 L), the foam containing 20% fiber residue (with a particle size of 28 mesh) achieved a maximum oil sorption of 15.9 $g \cdot g^{-1}$ after 48 h of exposure. The properties of S500 diesel (density = 850 $g \cdot L^{1}$ and viscosity ≈ 5 cSt at 25 °C) closely resemble those of the diesel used in the tests with the ZnO/HA-PC foam (Table IV). Consequently, for similar adsorbates, the performance of the ZnO/HA-PC foam significantly surpassed that of the foam synthesized by Martins et al. (2021).

Olivito et al. (2023) conducted a synthesis of bio-based polyurethane foams utilizing two distinct methodologies, producing materials designated as PU1 and PU2. The first synthesis

Table III. Physicochemical properties of the saline water used in the sorption tests.

Parameters	Seawater
Temperature (°C)	24.00 ± 1.00
pH	8.30 ± 0.11
Turbidity (NTU)	17.20 ± 0.09
Conductivity ($mS \cdot cm^{-1}$)	45.32 ± 1.12
Salinity (‰)	38.00 ± 1.00
Density ($g \cdot L^{-1}$)	1018 ± 2.00

yielded a foam with pore density of 10 pores per mm², whereas the second resulted in a greater pore density of 14 pores per mm². In a multicomponent system simulating diesel contamination in water (80 $g{\cdot}L^{-1}$), PU1 and PU2 demonstrated remarkable absorption capabilities, capturing 62 $g{\cdot}g^{-1}$ and 65 $g{\cdot}g^{-1}$ of diesel, alongside 4 $g{\cdot}g^{-1}$ and 2 $g{\cdot}g^{-1}$ of water, respectively. These findings suggest that an increase in both the quantity and volume of pores might significantly enhance the efficacy of oil recovery from aqueous environments.

The amounts of seawater and oil absorbed in the second system (8% (v/v) of S46 lubricating oil spilled into seawater) were very similar for the Un-PC foam. Although the modified foam sorbed approximately 130% more seawater than Un-PC did, the amount of S46 lubricating oil sorbed by ZnO/HA-PC increased by approximately 444%.

In the third system (8% (v/v) of 20W40 engine oil spilled into seawater), the ZnO/HA-PC foam produced the best results. There was an undesired increase in seawater sorption (compared with unaltered foam). However, there was also an outstanding 950% increase in 20W40 engine oil sorption. Un-PC foam was practically unable to sorb seawater or oil.

Tomon et al. (2024) developed a coconut oil-based polyurethane foam and assessed its capacity for oil and water recovery. In a medium containing only engine oil with density (830 $g{\cdot}L^{-1}$) and viscosity (494,000 cP) similar to the 20W40 engine oil (Table IV), the foam was capable of recovering up to 15 g of oil for each gram of foam

Table IV. Physicochemical and rheological properties of the oils used in the sorption tests.

Oil	Temperature[1] (°C)	Kinematic viscosity[2] (cSt)	Kinematic viscosity[3] 40 °C (cSt)	Density[4] ($g{\cdot}L^{-1}$)
Diesel	23.00 ± 1.00	5.02 ± 0.08	4.00 ± 0.15	839.00 ± 15.00
S46 lubricating	23.00 ± 1.00	97.00 ± 0.18	46.00 ± 0.10	858.00 ± 07.00
20W40 engine	23.00 ± 1.00	372.00 ± 0.88	120.00 ± 1.02	886.00 ± 12.00

[1]Room temperature on the day of sorption tests; [2]calculated viscosity at room temperature; [3]viscosity calculated at 40 °C (ASTM 2024); [4]density measured at room temperature.

Table V. Sorption test results for multicomponent systems containing seawater-oil.

Sorption ($g{\cdot}g^{-1}$)	**Seawater**		**Diesel**	
	Un-PC	ZnO/HA-PC	Un-PC	ZnO/HA-PC
	15.78^{a} ± 0.51	4.37^{b} ± 0.20	30.44^{A} ± 1.86	25.19^{B} ± 0.99
Sorption ($g{\cdot}g^{-1}$)	**Seawater**		**S46 lubricating oil**	
	Un-PC	ZnO/HA-PC	Un-PC	ZnO/HA-PC
	4.46^{b} ± 0.22	10.25^{a} ± 0.10	4.26^{B} ± 0.15	23.16^{A} ± 0.19
Sorption ($g{\cdot}g^{-1}$)	**Seawater**		**20W40 engine oil**	
	Un-PC	ZnO/HA-PC	Un-PC	ZnO/HA-PC
	0.09^{b} ± 0.00	0.45^{a} ± 0.02	1.38^{B} ± 0.04	14.50^{A} ± 0.04

Equal lowercase (seawater) and uppercase (oils) letters on the same line indicate no statistical difference in the Tukey test with a significance level of 5%.

used. These findings demonstrate an increase of over 500% in oil recovery compared to the unmodified foam, which only achieved 2.5 $g \cdot g^{-1}$. The results obtained from the ZnO/HA-PC foam surpassed those of Tomon et al. (2024) for oil with comparable properties. However, unlike the ZnO/HA-PC foam, the modified foam of Tomon et al. (2024) exhibited a reduction in seawater sorption by approximately 33% compared to the unmodified version.

Viscosity plays a fundamental role when the systems are compared. The (kinematic) viscosities (determined at 40 °C according to ASTM D445 (ASTM 2024)) of S46 lubricating oil (46 cSt) and 20W40 engine oil (120 cSt) are approximately 11 and 30 times greater than the viscosity of diesel (4 cSt), respectively. In the system with diesel, both foams had excellent performance in capturing the oil, as it flowed easily into the pores. This ease of flow made the modifications secondary to the sorption process. However, when more viscous oils were used, the flow difficulty caused by the increase in viscosity caused the surface modifications to become of primary importance in transporting the oils into the pores.

The findings of this work are aligned with the literature. Joy et al. (2020) evaluated the sorption of diesel and distilled water using new pure polyurethane foam and new polyurethane foam modified with MoS_2. The selectivity for diesel over water for the unaltered and modified foams was 38.87% and 91.82%, respectively. In the present work, the selectivity for diesel over seawater reached 65.8% and 85.2% for Un-PC and ZnO/HA-PC, respectively.

Wu et al. (2023), using a new polyurethane foam with a multifunctional arrangement of lignin grafted with SiO_2 nanoparticles, obtained 99% recovery of both n-hexane and chloroform poured into water. Zhang et al. (2022) modified a new polyurethane by depositing ferric oxide nanoparticles, graphene oxide, and phytic acid. A 98.9% recovery of n-hexane in water was obtained. The values of both studies are greater than those reported for the recoveries of the S46 lubricating oil (88%) and engine oil 20W40 (55%) used in this work. However, the difference in viscosity between pure substances and industrial oils is a factor that must be considered.

Joy et al. (2020) evaluated the sorption capacity of 2T oil in a (distilled) water-oil system with a new polyurethane foam unmodified and modified with MoS_2. The 2T oil has characteristics similar to those of the 20W40 engine oil, with a kinematic viscosity close to 95 cSt. The new polyurethane foam was able to sorb 60.65% of its own mass in 2T oil, whereas the modified polyurethane foam was able to sorb 255.79%, an increase of 321.75%. This increase was much lower than that observed between Un-PC and ZnO/HA-PC (950% increase in sorption of 20W40 engine oil in the third multicomponent system).

Sorption kinetics in water-oil system

The sorption of diesel and S46 lubricating was fast and practically reached stability within 25 s of exposure (Figure 5b and Figure 5d). 20W40 engine oil (~120 cSt) is approximately 30 times more viscous than diesel (~4 cSt), and as expected, its sorption stability took longer: approximately 30 s (Figure 5f).

The behavior for seawater sorption showed different results for each type of system. In the first multicomponent system (8% (v/v) of diesel spilled into seawater), at approximately 15 s, the amount of seawater sorbed was practically stable (Figure 5a), in contrast with the diesel sorption, which continued to increase until reaching stability at approximately 25 s (Figure 5b). This result indicates that in the competition for spaces in the pores and channels, there was a preference for oil due to the selectivity induced by surface modifications.

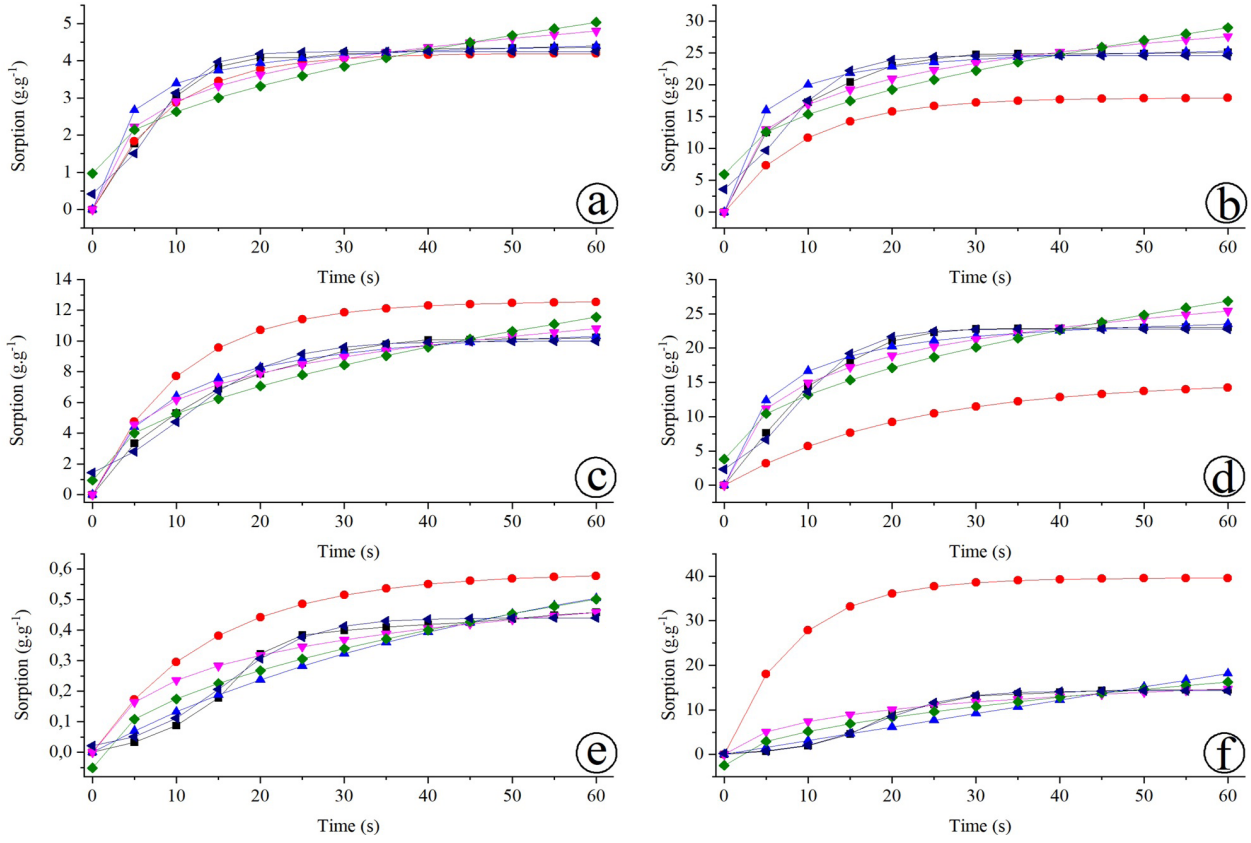

Figure 5. —■— Experimental data for the sorption of seawater (a, c, and e) and oils (b, d, and f), respectively, in the multicomponent systems seawater-diesel (a and b), seawater-S46 lubricating (c and d), and seawater-20W40 engine oil (e and f). Data estimated using the —●— Lagergren (Pseudo-first-order), —▲— Ho & McKay (Pseudo-second-order), —▼— Elovich (Chemisorption), —♦— Weber and Morris (Intraparticle diffusion), and —◄— Verhulst (Logistic) kinetic models.

At 5 s, approximately 47% of the initially spilled diesel was already sorbed in the ZnO/HA-PC foam (Figure 5b). At 25 s, more than 91% of the diesel had already been recovered. From 25 s onward, the sorption rate remained low until stabilization, with approximately 95% oil recovery occurring at 60 s. Among the kinetic models used to fit the experimental data, the pseudo-first-order (Lagergren 1898) and logistic (Bacaër 2011) models best described the sorption behavior for seawater, and the pseudo-second-order (Ho & McKay 1999) and logistic (Bacaër 2011) models best described the sorption behavior for diesel.

Olivito et al. (2023) developed bio-based polyurethane foams using two distinct methods, resulting in products designated as PU1 and PU2. The kinetic studies on the recovery of diesel and gasoline spilled in water indicated that the pseudo-second-order model most accurately represented the sorption behavior of the oils, as evidenced by R^2 values exceeding 0.99 for both diesel and gasoline sorption in both PU1 and PU2 foams.

In the second multicomponent system (8% (v/v) of S46 lubricating oil spilled into seawater), the seawater sorption continued to increase (Figure 5c) even after the oil sorption stabilized (Figure 5d). While the stability of the oil sorption occurred at approximately 25 s, for the seawater, it occurred only at approximately 40 s. This may have occurred due to the incomplete penetration of the oil into all the foam pores, especially those

located more in the center of the foam blocks. The modifications made it possible to increase the surface selectivity for oily structures as well as increase the intermolecular forces that attract the most viscous oils to the interior of the foam pores by capillarity. However, if the water penetrates faster than the oil, that pore may be exclusively filled by water over time since the fluids are incompatible in terms of mixing. For S46 lubricating sorption (Figure 5d), after just 10 s, more than 55% of the initially spilled oil was recovered. After 30 s and above, the amount of oil sorbed was practically constant, reaching 88% recovery at 60 s. The pseudo-second-order (HO & McKay 1999) and logistic (Bacaër 2011) kinetic models best described the sorption behavior of both the seawater and the S46 lubricating oil.

In the third multicomponent system (8% (v/v) of 20W40 engine oil spilled into seawater), the seawater and the 20W40 engine oil sorption rates were lower than those reported in other systems because of the difficulty in fluid flow caused by the higher viscosity of the engine oil. Both the seawater and the 20W40 engine oil showed sorption profiles similar to a logarithmic function (Figure 5e and Figure 5f). After 25 s, the sorption of both fluids drastically decreased, essentially stabilizing at 50 s, reaching a 55% recovery of the oil initially spilled. The logistic (Bacaër 2011) kinetic model was the one that best described the sorption behavior of both the seawater and the 20W40 engine oil.

When the pseudo-first-order model satisfactorily fits the experimental data, it indicates the presence of a reversible mass transport system where physical sorption is the predominant transport mechanism. On the other hand, a good fit of the pseudo-second-order model indicates that there is both physical and chemical sorption and that they control the transport mechanism (Blaquera et al. 2023).

For both the diesel and the S46 lubricating oil sorption, the pseudo-first-order model underestimated the amount of oil recovered at equilibrium (q_e) by the ZnO/HA-PC foam by approximately 28% and 39%, respectively (Table VI). In contrast, the model overestimated the 20W40 engine oil sorption at equilibrium by more than 172%.

The pseudo-second-order kinetic model showed excellent suitability for both the diesel and the S46 lubricating oils (Table VI), with variations of +6% and +2%, respectively, between the experimental ($Q_{e(exp.)}$) and mathematically determined ($Q_{e(calc.)}$) data. The model was not able to fit the experimental data of 20W40 engine oil sorption ($R^2 < 0.1$).

The elevated coefficient of determination (R^2) observed for the pseudo-second-order kinetic model allied with the results for the pseudo-first-order model indicates that both physical and chemical sorption are present (Piperopoulos et al. 2018, Blaquera et al. 2023) and rule the mass transport of diesel and S46 lubricating oils into the foam pores. Since chemisorption proved to be a relevant part of mass transport, the Elovich model should be used to collaborate with the understanding of this transport phenomenon.

In the Elovich kinetic model, α is the initial sorption rate, whereas β is related to the surface size of the foam and the activation energy used to promote chemisorption (Yaneva et al. 2012). The surface area of the foam and its pores (sites) are considered to be energetically heterogeneous. That is, the adsorption sites have different sizes and amounts of energy to interact with the fluid molecules to be adsorbed (Roginsky & Zeldovich 1934). Table VI shows the tendency between the increase in oil viscosity and the increase in the β parameter, *i.e.*, with increasing oil viscosity (diesel > S46 lubricating > 20W40 engine), the need for the area available on the surface of

Table VI. Calculated and estimated kinetic parameters for each kinetic model studied.

Kinetics	Parameters	Seawater[1]	Diesel	Seawater[2]	S46 Lub.	Seawater[3]	20W40 eng.
Pseudo-First-Order (Lagergren)	k_1 ($g \cdot g^{-1} \cdot s^{-1}$)	0.115	0.105	0.009	0.004	0.070	0.121
	$^4Q_{e(exp.)}$ ($g \cdot g^{-1}$)	4.360	25.086	10.230	24.985	0.458	14.519
	$^5Q_{e(calc.)}$ ($g \cdot g^{-1}$)	4.197	17.943	12.568	15.138	0.586	39.583
	R^2	0.977	0.940	0.979	0.830	0.966	0.727
	SSR	0.460	569.823	69.035	1164.741	0.242	7651.029
Pseudo-Second-Order (Ho & McKay)	k_2 ($g \cdot g^{-1} \cdot s^{-1}$)	0.057	0.011	0.010	0.007	0.011	< 0.001
	$^4Q_{e(exp.)}$ ($g \cdot g^{-1}$)	4.360	25.086	10.230	24.985	0.458	14.519
	$^5Q_{e(calc.)}$ ($g \cdot g^{-1}$)	4.667	26.668	11.755	25.561	1.151	718.382
	R^2	0.992	0.994	0.975	0.982	0.194	0.000
	SSR	0.952	22.622	3.191	31.768	0.033	69.303
Chemisorption (Elovich)	α ($g \cdot g^{-1} \cdot s^{-1}$)	1.451	8.878	2.352	6.441	0.063	1.870
	β ($g \cdot g^{-1}$)	0.915	0.162	0.367	0.164	7.345	0.220
	R^2	0.938	0.950	0.983	0.949	0.867	0.837
	SSR	1.182	24.976	3.257	36.044	0.053	73.692
Intraparticle diffusion (Weber & Morris)	k_d ($g \cdot g^{-1} \cdot s^{-0.5}$)	0.525	2.971	1.369	2.973	0.071	2.411
	C ($g \cdot g^{-1}$)	0.972	5.942	0.937	3.809	-0.051	-2.434
	R^2	0.816	0.831	0.939	0.850	0.897	0.890
	SSR	3.797	109.558	7.485	94.908	0.036	43.983
Logistic (Verhulst)	a ($g \cdot g^{-1}$)	4.250	24.573	9.987	22.771	0.440	14.279
	b	9.240	5.866	5.945	8.785	19.796	50.300
	c (s^1)	0.325	0.267	0.167	0.257	0.190	0.216
	R^2	0.999	0.999	0.999	0.998	0.982	0.998
	SSR	0.347	26.159	3.455	9.089	0.004	1.137

[1]Seawater from the seawater-diesel system; [2]seawater from the seawater-S46 lubricating oil system; [3]seawater from the seawater-20W40 engine oil system; [4]oil sorption at equilibrium – experimental data; [5]oil sorption at equilibrium – calculated data.

the foam and the energy for chemisorption also increase. This tendency, allied with the R^2 performance, reinforces that chemisorption is an essential (and rate-limiting) part of the mass transport process.

Yaneva et al. (2012) studied the sorption of nitrophenols in expanded perlite. After observing that the pseudo-second-order model had adequate suitability for the experimental data, the Elovich kinetic model was used and revealed that the increase in the β parameter was associated with the increased activation energy and surface area required for chemisorption. The results indicated an agreement between the pseudo-second-order and Elovich models, both with high R^2 values.

Blaquera et al. (2023) studied engine oil recovery in a water-oil system using calcium stearate-coated kapok fibers. The pseudo-second-order model showed the best results in modeling the experimental data ($R^2 > 0.99$), followed by the good performance of Elovich's

model ($R^2 > 0.86$), indicating that chemisorption had a strong influence on mass transport. A high α value was also observed.

In this work, the three oils tested also presented high values of Elovich's α parameter, which is characteristic of rapid oil sorption in the initial seconds of contact (Yaneva et al. 2012, Blaquera et al. 2023). As shown in Figure 5 and Table VI, the increase in oil viscosity reduced the α parameter because it reduced the slope of the initial oil sorption curves and, consequently, the initial sorption rate (α).

Parameter C from the Weber and Morris equation (Table I) corresponds to the intercept of the linear equation. This equation models intraparticle diffusion, which refers to the transport of dispersed oil in the liquid phase (seawater) to the surface and pores of modified polyurethane foam (Nwadiogbu et al. 2016, Blaquera et al. 2023). The intraparticle diffusion model assumes that adsorption is controlled in three stages: (I) rapid and external adsorption on the adsorbent surface; (II) gradual adsorption, where intraparticle diffusion is the limiting step; and (III) the final equilibrium stage, where intraparticle diffusion begins to decrease because of the low concentration of adsorbate in the liquid and the low availability of active sites (Weber & Morris 1963). When the intercept C tends to zero (remaining only the equation's angular coefficient), fluid diffusion in the pores tends to be rate limiting (Blaquera et al. 2023). That is, if $C \rightarrow 0$, fluid penetration into the foam pores is the most relevant step for explaining the transport mechanism. Otherwise, if the value of the C parameter is elevated, the sorption mechanism presents a high boundary layer effect that occurs mainly on the surface of the foam and controls the limiting rate of mass transport (Piperopoulos et al. 2018, Blaquera et al. 2023).

As shown in Table VI, the values of parameter C for the sorption of diesel, S46 lubricating, and 20W40 engine oils were elevated, as were their respective R^2. The good regression values indicate the presence of the intraparticle diffusion phenomenon in the recovery of spilled oils through the ZnO/HA-PC foam. Furthermore, the high values of C prove the influence of the first stage in controlling the sorption mechanism: rapid and external adsorption on the adsorbent surface. This means that not only the intraparticle diffusion mechanism but also oil sorption on the foam surface is rate limiting.

Nwadiogbu et al. (2016) reported that both surface sorption and intraparticle diffusion were rate-limiting in the sorption process of spilled crude oil in water when corncobs were used as adsorbents. Blaquera et al. (2023), using Kapok fibers coated with calcium stearate, recovered engine oil spilled in water. High values of the C parameter and R^2 were obtained, indicating that surface sorption was the predominant diffusion mechanism in the water-oil system studied.

Verhulst's logistic model presented the best fit for the experimental data obtained after the sorption of the three oils tested in this work. This model was originally used in the study of population growth. After decades of adaptation, it has been used in different applications, such as monitoring COVID-19 (Souza & Kock 2022) and autocatalytic chemical reactions (Schuster 2019), for example. The logistic growth curve is sigmoid with a start that resembles an exponential function and then, after having passed an inflection point, becomes saturated (Schuster 2019), exactly as shown in Figure 5.

The sorption modeling of all three oils resulted in very high regressions ($R^2 > 0.99$), indicating excellent suitability of the logistic model for the experimental data (Table VI). The good predictability of this nonlinear model is directly associated with its low complexity owing

to the lack of nullity in its parameters (a, b, and c ≠ 0). Otherwise, in the case of nullity of any of them, there would be a very low correlation between the model and the experimental data.

Knapik & Stopa (2018) used an adapted logistic model to fit the data obtained from oil sorption in water-oil systems applying sunflower pith as an adsorbent. Among the oils tested were diesel and 15W40 engine oils. The logistic model showed a high correlation ($R^2 > 0.98$) and was superior to the other models in all cases, such as the pseudo-second-order model, for example ($R^2 > 0.72$). Other adaptations of the kinetic logistic model have been reported for the sorption of dyes and organic matter, among others, through the use of non-conventional adsorbents (Chu 2020, Volikov et al. 2023).

Retention-dripping kinetics

In a system with an excess of adsorbate, the saturation point of the adsorbent will eventually be reached. For the foams modified in this work, once they become saturated with oils recovered from the sea, they need to be lifted and compressed over a tank for the desorption and recovery of the sorbed fluids. After this process, the foams can be reused in the sorption/desorption cycles until they are exhausted or until all spilled oils are completely recovered. However, if a significant portion of the fluids is desorbed during the movement of the saturated foams (for example, during hoisting), their effectiveness as an adsorbent material becomes impractical.

To evaluate this critical parameter, a retention-dripping kinetic study was conducted using the equations (Equations 6-8) established by Bazargan et al. (2015a). This study analyzed the experimental data obtained from oil sorption in a single-component system with either diesel, S46 lubricating oil, or 20W40 engine oil. The parameters calculated through nonlinear regression, based on the experimental data of the desorption kinetics presented in Figure 6, are summarized in Table VII.

The k coefficient (Kammam) is essential for interpreting the results of the kinetic profile. According to Bazargan et al. (2015a), a smaller Kamaan coefficient indicates that the sorbate is lost more slowly, resulting in less dripping. The values of the k coefficient presented in Table VII support this assertion. For instance, the dripping rate of diesel ($k = 0.005\ s^{-1}$) was very slow, whereas S46 lubricating oil ($k = 0.015\ s^{-1}$) and 20W40 engine oil ($k = 0.019\ s^{-1}$) exhibited much faster dripping rates.

Bazargan et al. (2015a) base their analysis on the fact that the k coefficient in Equations 6 and 7 mathematically governs the curvature of the kinetic profile. When there is minimal dripping - indicating low desorption - the curvature is minor. In contrast, intense dripping, which results in significant fluid loss due to desorption, produces a steeper curve during the phase of greatest loss, as illustrated in Figure 6. The connection between increased dripping, a higher k coefficient, and a steeper curvature of the kinetic shown in Figure 6 and Table VII was also observed and reported by Bazargan et al. (2015a), yielding similar results and k values.

Condurache et al. (2022) suggest that fluids with higher densities exhibit a higher k coefficient than those with lower densities. Based on the densities and kinematic viscosities for diesel, S46 lubricating oil, and 20W40 engine oil, as reported in Table IV, this inference is supported. The order of increasing density, viscosity, dripping (desorption), and k coefficient was as follows: diesel > S46 lubricating oil > 20W40 engine oil.

Another important aspect of the k coefficient is its invariance between normalized and non-normalized equational models. The k values reported in Table VII are similar for

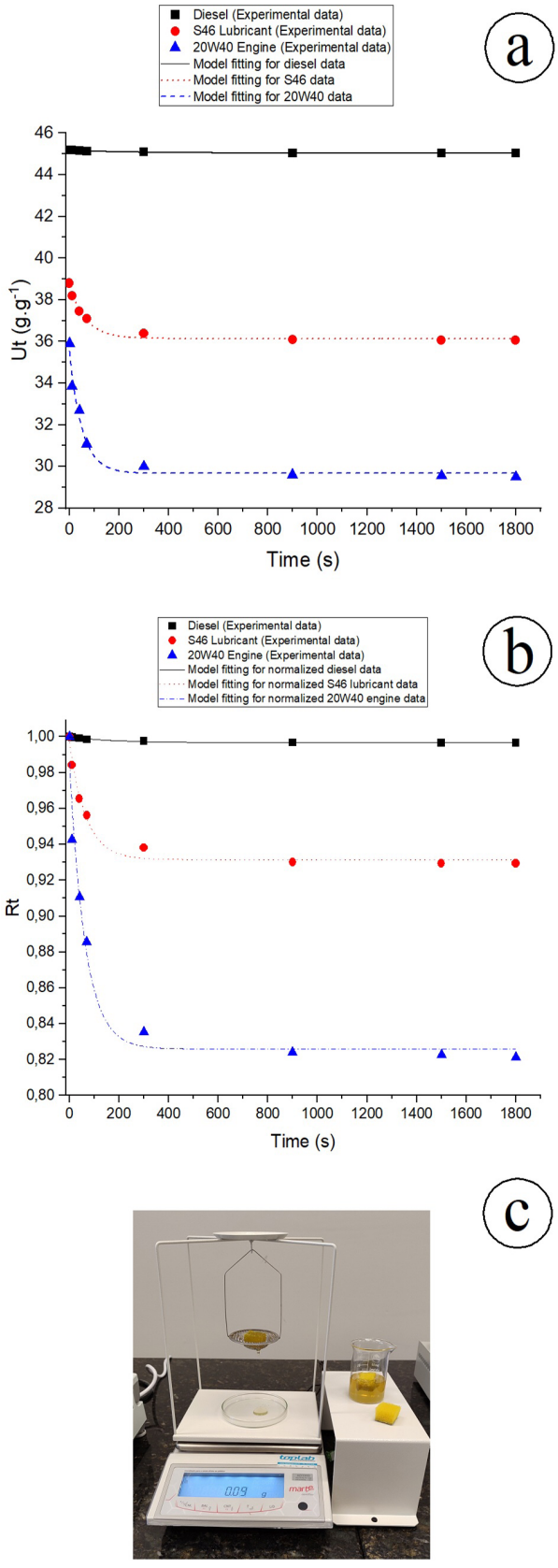

Figure 6. Desorption kinetic profiles of oils sorbed by ZnO/HA-PC foam fitted using both the non-normalized (a) and normalized (b) equations from Bazargan et al. (2015a). Analytical balance equipped with a mesh basket support used to collect the experimental data (c).

the desorption of the same fluid, regardless of whether the normalized or non-normalized equation is used, which indicates that the curvature remains consistent. This observation aligns with findings from Bazargan et al. (2015a) and Condurache et al. (2022).

By adding the values of U_L and U_e, the maximum sorption capacity of the adsorbent can be estimated. While U_L refers to the fraction of fluid that was desorbed (through dripping), U_e is the fraction of fluid that remains sorbed on the adsorbent material after a long period. The sum of U_L and U_e, as reported in Table VII, shows values very close to the experimental results.

At the initial time (t = 0 s), it is assumed that there is no loss due to desorption, meaning this is when the adsorbent material exhibits its highest sorption capacity. In a single-component system, the maximum sorption capacity (t = 0 s) of the ZnO/HA-PC foam was found to be 45.20 $g \cdot g^{-1}$, 38.79 $g \cdot g^{-1}$, and 35.91 $g \cdot g^{-1}$, for diesel, S46 lubricating oil, and 20W40 engine oil, respectively. Comparing these experimental values with those estimated ($U_L + U_e$) by the non-normalized model presented in Table VII, the model underestimated the maximum sorption by only 0.04%, 0.31%, and 1.09% for diesel, S46 lubricating oil, and 20W40 engine oil, respectively. These highly accurate results are supported by a high coefficient of determination (R^2) and low chi-square (χ^2) value reported for the models in Table VII.

The same principles and observations can be applied for the normalized model and its results. The closer the sum of $R_L + R_e$ is to 1 (or 100%), the better the model represents the

Table VII. Parameters for unsteady-state retention models.

Kinetics	Parameters	Diesel	S46 lubricating oil	20W40 engine oil
$U_t = U_L e^{-kt} + U_e$	U_L ($g \cdot g^{-1}$)	0.143	2.532	5.864
	U_e ($g \cdot g^{-1}$)	45.045	36.136	29.662
	$U_L + U_e$ ($g \cdot g^{-1}$)	45.188	38.668	35.526
	k (s^{-1})	0.005	0.015	0.019
	R^2	0.979	0.985	0.979
	χ^2	$1.219 \cdot 10^{-4}$	$2.233 \cdot 10^{-2}$	$1.655 \cdot 10^{-1}$
$R_t = R_L e^{-kt} + R_e$	R_L	0.003	0.065	0.159
	R_e	0.996	0.931	0.825
	$R_L + R_e$	0.999	0.996	0.984
	k (s^{1})	0.005	0.015	0.019
	R^2	0.979	0.985	0.976
	χ^2	$5.939 \cdot 10^{-8}$	$1.498 \cdot 10^{-5}$	$1.474 \cdot 10^{-4}$

experimental data. R_L can be interpreted as 1 - R_e. When t = 0 s, the Equation 7 results in R_t = 1, meaning 100% of the fluid is adsorbed onto the adsorbent material. As time progresses (t > 0 s), R_L is expected to be smaller than R_e for an effective adsorbent. Conversely, if R_L exceeds R_e, the adsorbent is deemed inefficient, as it loses more than 50% of the fluid that was initially sorbed.

Condurache et al. (2022) investigated the sorption of oil spills using wool fibers through the unsteady-state retention model developed by Bazargan et al. (2015a). The kinetic study of the desorption of dodecane and 15W40 engine oil produced similar results and kinetic interpretations as those observed for diesel and 20W40 engine oil in this study.

The results of oil sorption on ZnO/HA-PC foam indicated that, even for denser and more viscous oils, such as 20W40, the fluid loss due to desorption (U_L) was relatively low, with a maximum loss of 16.51%. This indicates that more than 83% of the 20W40 engine oil remained sorbed on the foam (U_e), even after being exposed to conditions favoring dripping for 1800 s. The results for S46 lubricating oil and diesel are even more impressive: the loss for S46 lubricating oil was only 6.55%, leaving 93.45% remaining, while diesel had a minimal loss of 0.32%, resulting in 99.68% still retained.

The equations developed by Bazargan et al. (2015a) and proposed by Bazargan et al. (2015b), which aim to enhance the standardization of reports on adsorbent materials used for spilled oils (ASTM 2017), have proven to be effective and highly accurate for different types of adsorbents.

Oil desorption and foam reuse

Different techniques have been reported in the literature for the desorption of oils that have been sorbed onto porous structures. These techniques include centrifugation (Condurache et al. 2022), vacuum filtration (Lu et al. 2019), and mechanical squeezing (Udayakumar et al. 2021, Rocha et al. 2023a). In the context of oil spills in the ocean, which is the focus of this study, tankers can be effectively applied to store oils that have been desorbed from foams. Among the available methods, mechanical squeezing

stands out as one of the most economically and strategically viable desorption techniques.

In this technique, the oil - and water - saturated foams are lifted and compressed over the ship's tank to facilitate oil recovery. The cycle of sorption and desorption continues until the foam's oil separation capacity is fully exhausted or there is no more oil available for sorption. Based on this approach, the oils and seawater sorbed by the ZnO/HA-PC foams used during the sorption tests in multicomponent systems were desorbed using mechanical compression with a vise. The evaluation of their reusability was conducted throughout the cycles, and the results are summarized in Figure 7.

For both seawater and oil (including diesel, S46 lubricating oil, and 20W40 engine oil) that were sorbed by ZnO/HA-PC, there was no statistically significant change (p-value < 0.05) observed over 50 sorption and desorption cycles. Additionally, the volume of the foam cubes was measured using a digital caliper and showed no significant variation throughout the cycles. These results demonstrate the considerable reuse potential of the modified foams.

Li et al. (2015) investigated the combined modification of ZnO and HA in newly synthesized polyurethane foams. They tested the foams for their sorption capacity in a single-component system using different types of oil (including diesel, pumping oil, and petroleum). Their findings indicated that the foams started to deteriorate and lose their reusability for all the tested oils only after 60 cycles of sorption and desorption.

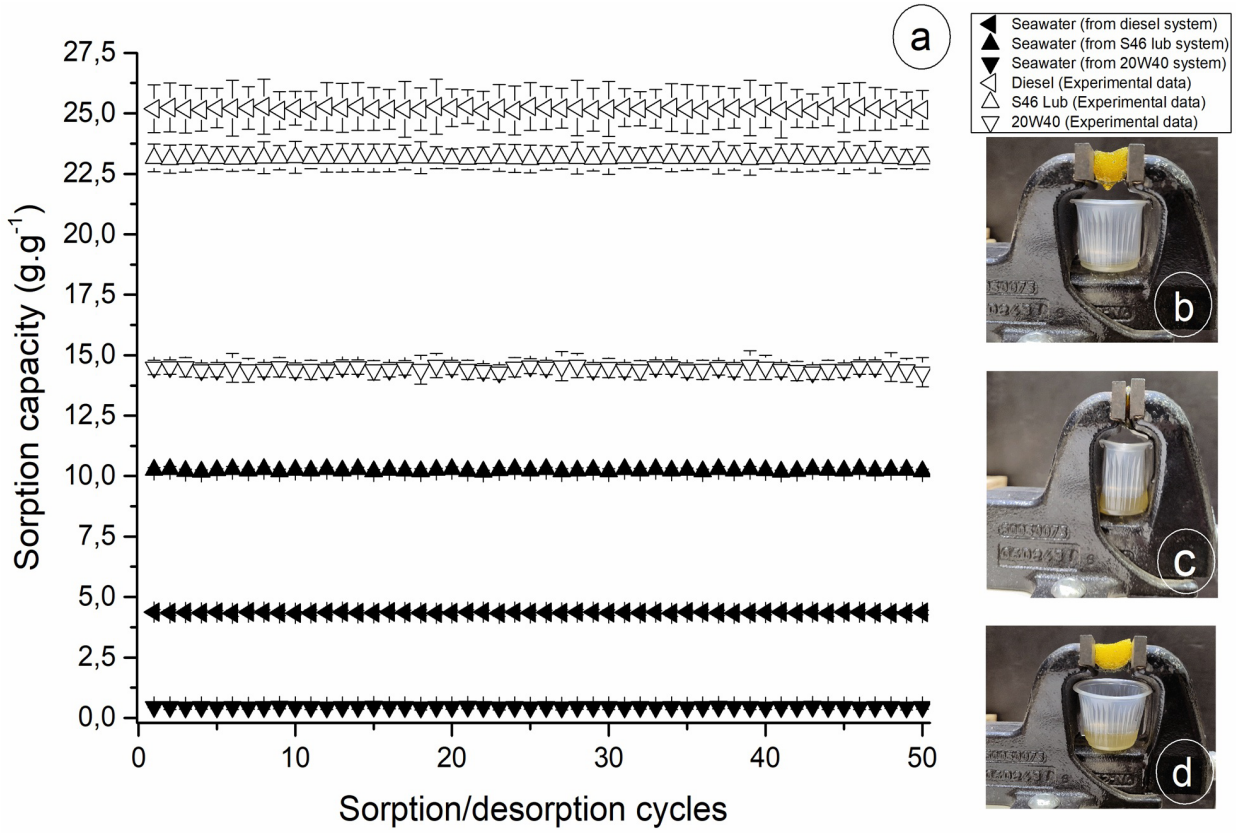

Figure 7. Sorption and desorption cycles of ZnO/HA-PC foam in seawater-oil multicomponent systems (a). Initial (b), middle (c), and final (d) stages of mechanical compression in a vise for desorbing the fluids absorbed by the foam.

Tomon et al. (2024) synthesized a coconut oil-based polyurethane foam and evaluated its reusability for the recovery of oil (20 cycles) and water (10 cycles). In a medium containing only engine oil with density (830 $g{\cdot}L^{-1}$) and viscosity (494,000 cP) similar to the 20W40 engine oil (Table IV), a relative consistency was noted in the sorption capacity across the different cycles, indicating that the foam was capable of being reused multiple times. In contrast, for seawater, Tomon et al. (2024) reported a slight increase in sorption across the cycles; however, this increase was insignificant, not exceeding 1.5 $g{\cdot}g^{-1}$. The sorption/desorption cycles of 20W40 engine oil (as well as for seawater) for the ZnO/HA-PC foam demonstrated less fluctuation compared to the polyurethane foam modified by Tomon et al. (2024).

The structural integrity of the ZnO/HA post-consumer foams is responsible for the long sorption and desorption cycle (Figure 7). The same was observed by Li et al. (2015) for newly synthesized foams. This suggests that the "post-consumer condition" did not affect the results, leading to outcomes comparable to those of new foams.

To support this finding, Rocha et al. (2023a) compared the sorption capacity of new polyurethane foams modified separately with ZnO and HA. The results for the new foams modified with HA were insignificant. However, the sorption results for the new foams modified with ZnO closely matched those obtained by Li et al. (2015) for new polyurethane foams that had simultaneous ZnO and HA modification. Notably, the ZnO-modified foams from Rocha et al. (2023a) could only sustain 10 cycles of sorption and desorption. In contrast, the current study demonstrated that ZnO/HA-modified post-consumer foams could endure 50 cycles, aligning with Li et al. (2015), which reported over 50 cycles for new polyurethane foams.

Segovia et al. (2011), Agrawal et al. (2017) and Trino et al. (2018) theorize that the increased structural integrity observed in foams modified with ZnO/HA compared to those modified with ZnO alone may be attributed to the protective film coating provided by HA. In the case of modifications using only ZnO, the synthesized oxide rods can penetrate the surface and nanopores of the polyurethane (Rocha et al. 2023a). During the sorption and desorption cycles, these rods may break and detach from the structure, compromising its integrity. The HA coating develops as a film deposition (Li et al. 2015), serving as multiple layers that protect not only the polyurethane structure but also the ZnO rods (see Figure 2d). This enhanced protection increases both the resistance of the rods and the durability of their hydrophobic and lipophilic properties.

Perspectives for the practical application of ZnO/HA-PC

When oil spills occur at sea, several techniques can be employed for remediation. Each one has its advantages and disadvantages that should be considered when determining the most effective approach, whether used alone or in combination with others. The most commonly utilized and documented techniques include in-situ burning (Li et al. 2020), skimming using pumps (Li et al. 2016), and chemical dispersion (Silva et al. 2022).

The in-situ burning of spilled oil faces two significant challenges: the necessity of having a thick oil layer to sustain the flame and the emission of toxic gases that pose risks to both workers involved in the cleanup and the surrounding ecosystem (Li et al. 2020). Furthermore, the use of skimmers for pumping is often ineffective in rough seas and high winds, and it can also lead to secondary contamination due to its oleophilic structures (Piao et al.

2023). Chemical dispersants are employed to break down dense layers of oil into smaller droplets that can be more readily degraded. However, as its name implies, this technique tends to disperse and spread oil droplets across multiple biomes before they undergo complete degradation (Silva et al. 2022).

Research has demonstrated that the size and movement of spilled oil in the marine environment, including factors like the area it spreads over and the rate of spreading, as well as the effects of the weathering process - such as evaporation, dissolution, and dispersion - can significantly influence the extent of subsequent damage (Lee et al. 2023), directly affecting the effectiveness of traditional remediation methods (Piao et al. 2023).

Etkin & Nedwed (2021) conducted a comprehensive study evaluating the effectiveness of mechanical recovery techniques employed in oil spill disasters over the past few decades. Their findings revealed that no more than 6% of the oil spilled was effectively recovered. If evaporation, dissolution, and dispersion are included in the oil availability equation, this recovery reaches 15%. These findings underscore the significant challenges posed by traditional recovery methods and highlight the urgent need for alternative strategies to mitigate the impacts of oil spills.

In the context of this investigation, the polyurethane foam examined herein emerges as a viable alternative to conventional methodologies, and may also serve as a complementary approach to these established techniques.

The ZnO/HA-PC foam exhibited a density of 25 $g{\cdot}L^{-1}$ (Table II), which was significantly lower than that of seawater, measured at 1018 $g{\cdot}L^{-1}$ (Table III). Therefore, as expected, the foams remained floating in all tests due to the density differential. Even after absorbing oils to saturation, the foam + oil maintained a density that was still less than that of seawater, ensuring it stayed afloat. In contrast to skimmers and booms, which can lose efficiency due to wind force and sea movement (Piao et al. 2023), ZnO/HA-PC foams are able to adapt to the dynamics of waves while floating on the ocean's surface. This characteristic provides a considerable advantage in their application. Additionally, debris has minimal effect on the oil sorption efficiency of the foams, unlike skimmers that are prone to clogging.

Once the foams are saturated, they must be hoisted and compressed over a reservoir to desorb the retained oil and water. During the hoisting process, the primary concern is the desorption that occurs due to the movement of the foam before it reaches the collecting reservoir. In the retention-dripping kinetics study (Figure 6), the foams were saturated with oil and elevated, remaining in that position for up to 30 min. The results indicated that 99.68%, 93.45%, and 83% of diesel, S46 lubricating oil, and 20W40 engine oil, respectively, remained adsorbed to the foams even after 30 min suspended. These findings also support the potential application of the foams for oil spill recovery, as they demonstrate an ability to retain adsorbates even while in motion.

The results from the reusability tests (Figure 7) provide even more evidence supporting the application of foams in the recovery of oil spills in marine environments. Throughout the course of 50 sorption and desorption cycles, the ZnO/HA-PC foam demonstrated a remarkable ability to maintain a consistent sorption capacity. This finding suggests that the material can be effectively utilized multiple times, thereby promoting cost efficiency while utilizing a recycled material that incurs low acquisition and modification expenses.

CONCLUSIONS

The polyurethane foams obtained from discarded mattresses showed potential for recycling and reuse as adsorbent material for oil recovery in seawater spills. Through relatively low-cost modifications, the foams significantly enhanced their oil sorption capacity, achieving increases of up to 950%.

Among the linearized kinetic models analyzed, the logistic (Verhulst) and pseudo-second-order (Ho & McKay) models provided the best fit for the experimental data across all types of oils evaluated. It was observed that the viscosity of the oils had a significant impact on the results of all tests conducted.

The kinetic desorption tests showed that foams saturated with denser and more viscous oils exhibited a higher initial dripping rate and greater loss during desorption compared to foams saturated with less dense and viscous oils. Furthermore, the desorption and reuse tests demonstrated that the foams maintained a statistically consistent sorption capacity throughout the 50 cycles of sorption and desorption evaluated.

All the results presented in this work highlight the potential of using post-consumer polyurethane foams from mattresses as an alternative adsorbent material for recovering oil spills at sea. This approach utilizes one type of waste to address another, effectively tackling two seemingly unrelated issues to mitigate the environmental impact caused by industrial activities.

Acknowledgments

This work is supported by the Brazilian National Agency of Petroleum, Natural Gas, and Biofuels through the Human Resources Program PRH 44.1.

REFERENCES

ABERNATHY SA, GILLIAM JK & KLOUDA PJ. 1989. Drilling and Production Discharges and Oil Spills in the Marine Environment. Virginia: U.S. Department of The Interior. Available at: https://espis.boem.gov/Final%20Reports/4758.pdf. Accessed: 07 June 2025.

AGRAWAL N, MUNJAL S, ANSARI MZ & KHARE N. 2017. Superhydrophobic palmitic acid modified ZnO nanoparticles. Ceram Int 43: 14271-14276. http://dx.doi.org/10.1016/j.ceramint.2017.07.176.

ASTM - AMERICAN SOCIETY FOR TESTING AND MATERIALS. 2017. ASTM F726 – Standard Test Method for Sorbent Performance of Adsorbents for Use on Crude Oil and Related Spills. Philadelphia: ASTM International. http://doi.org/10.1520/F0726-17.

ASTM - AMERICAN SOCIETY FOR TESTING AND MATERIALS. 2023. ASTM D95 – Standard Test Method for Water in Petroleum Products and Bituminous Materials by Distillation. Philadelphia: ASTM International. http://doi.org/10.1520/D0095-23E01.

ASTM - AMERICAN SOCIETY FOR TESTING AND MATERIALS. 2024. ASTM D445 – Standard Test Method for Kinematic Viscosity of Transparent and Opaque Liquids (the Calculation of Dynamic Viscosity). Philadelphia: ASTM International. http://doi.org/10.1520/D0445-24.

BACAËR N. 2011. Verhulst and the logistic equation (1838). In: A Short History of Mathematical Population Dynamics (35-39). London: Springer. http://doi.org/10.1007/978-0-85729-115-8_6.

BAZARGAN A, SADEGHI H, GARCIA-MAYORAL R & MCKAY G. 2015a. An unsteady state retention model for fluid desorption from sorbents. J Colloid Interface Sci 450: 127-134. http://dx.doi.org/10.1016/j.jcis.2015.02.036.

BAZARGAN A, TAN J & MCKAY G. 2015b. Standardization of Oil Sorbent Performance Testing. J Test Eval 43: 1-8. http://doi.org/10.1520/JTE20140227.

BLAQUERA ALM, HERRERA MU, MANALO RD, MAGUYON-DETRAS MC, FUTALAN CCM & BALELA MDL. 2023. Oil Adsorption Kinetics of Calcium Stearate-Coated Kapok Fibers. Polymers (Basel) 15: e452. http://doi.org10.3390/polym15020452.

CADDEO S, BAINO F, FERREIRA AM, SARTORI S, NOVAJRA G, CIARDELLI G & VITALE-BROVARONE C. 2014. Collagen/Polyurethane-Coated Bioactive Glass: Early Achievements towards the Modelling of Healthy and Osteoporotic Bone. Key Eng Mater 631: 184-189. http://doi.org/10.4028/www.scientific.net/KEM.631.184.

CASSIE ABD & BAXTER S. 1944. Wettability of porous surfaces. Trans Faraday Soc 40: 546-551. https://doi.org/10.1039/TF9444000546.

CHOUDHURY ND, SAHA N, BHAUMIK S & KATAKI R. 2023. Production and evaluation of physicochemical, rheological, and tribological properties of *Cucurbita pepo L*. seed oil. Biomass Convers Biorefin 13: 1101-1114. http://doi.org/10.1007/s13399-020-01236-5.

CHU KH. 2020. Breakthrough curve analysis by simplistic models of fixed bed adsorption: In defense of the century-old Bohart-Adams model. Chem Eng J 380: e122513. http://doi.org/10.1016/j.cej.2019.122513.

COJOCARU C, MACOVEANU M & CRETESCU I. 2011. Peat-based sorbents for the removal of oil spills from water surface: application of artificial neural network modeling. Colloids Surf A: Physicochem Eng Asp 384: 675-684. http://www.doi.org/10.1016/j.colsurfa.2011.05.036.

CONDURACHE BC, COJOCARU C, SAMOILA P, IGNAT M & HARABAGIU V. 2022. Data-driven modeling and optimization of oil spill sorption by wool fibers: retention kinetics and recovery by centrifugation. Int J Environ Sci Technol 19: 367-378. https://doi.org/10.1007/s13762-021-03176-7.

COSTA RMD, HUNGERBÜHLER G, SARAIVA T, JONG G, MORAES RS, FURTADO EG, SILVA FM, OLIVEIRA GE, FERREIRA LS & JUNIOR FGS. 2017. Green polyurethane synthesis by emulsion technique: a magnetic composite for oil spill removal. Polímeros 27: 273-279. http://doi.org/10.1590/0104-1428.2397.

DAVE D & GHALY AE. 2011. Remediation Technologies for Marine Oil Spills: A Critical Review and Comparative Analysis. Am J Environ Sci 7: 423-440. http://doi.org/10.3844/ajessp.2011.423.440.

DORRAJI MSS, RASOULIFARD MH, SHAJERI M, ASHJARI HR, AZIZI M & RASTGOUY-HOUJAGHAN M. 2018. The role of prepared ZnO nanoparticles on improvement of mechanical and antibacterial properties of flexible polyurethane foams: experimental modeling. Polym Bull 75: 1519-1533. http://doi.org/10.1007/s00289-017-2105-0.

ENNACERI H, WANG L, ERFURT D, RIEDEL W, MANGALGIRI G, KHALDOUN A, KENZ AE, BENYOUSSEF A & ENNAOUI A. 2016. Water-resistant surfaces using zinc oxide structured nanorod arrays with switchable wetting property. Surf Coat Technol 299: 169-176. https://doi.org/10.1016/j.surfcoat.2016.04.056.

ETKIN DS & NEDWED TJ. 2021. Effectiveness of mechanical recovery for large offshore oil spills. Mar Pollut Bull 163: e111848. https://doi.org/10.1016/j.marpolbul.2020.111848.

FAKHAR A, MAGHAMI S, SAMETI E, SHEKARI M & SADEGHI M. 2020. Gas separation through polyurethane–ZnO mixed matrix membranes and mathematical modeling of the interfacial morphology. SPE Polymers 1: 113-124. https://doi.org/10.1002/pls2.10023.

FERREIRA I, FREIRE A, OLIVEIRA F & STEFFENS F. 2019. Uso de água do mar em tingimento têxtil para efeito de lavanderia: Uma alternativa prática e sustentável. Conference: 7º Simpósio Design Sustentável, p. 404-412. http://doi.org/10.5151/7dsd-2.2.037.

GRABOWSKI SJ. 2020. Understanding Hydrogen Bonds, 1st ed., London: Royal Society of Chemistry, 450 p.

GROTTO AC, HEMKEMEIER M & ROSSATO MV. 2020. Sustentabilidade no uso de poliuretano e reutilizações de aparas. Res Soc Dev 9: e99891110685. http://doi.org/10.33448/rsd-v9i11.10685.

GYAMFI BA, ADEDOYIN FF, BEIN MA, BEKUN FV & AGOZIE DQ. 2021. The anthropogenic consequences of energy consumption in E7 economies: Juxtaposing roles of renewable, coal, nuclear, oil and gas energy: Evidence from panel quantile method. J Clean Prod 295: e126373. http://doi.org/10.1016/j.jclepro.2021.126373.

HAMACHER C, FARIAS CO, ARAÚJO MP, PITTA JPMP, SANTOS CAP & SOARES MLG. 2022. Community-based assessment of marine resources contamination after a large-scale oil spill. An Acad Bras Cienc 94: e20211392. https://doi.org/10.1590/0001-3765202220211392.

HO YS & MCKAY G. 1999. A kinetic study of dye sorption by biosorbent waste product pith. Resour Conserv Recy 25: 171-193. http://doi.org/10.1016/S0921-3449(98)00053-6.

INOJOSA FCP, PEDROSA LF, CASTRO MCT, AMORIM MN, FRANÇA MR & MOURA RN. 2022. Lessons learned from a mystery oil spill that hit the Brazilian coast in 2019. An Acad Bras Cienc 94: e20210309. https://doi.org/10.1590/0001-3765202220210309.

JOY J, ABRAHAM J, SUNNY J, MATHEW J & GEORGE SC. 2020. Hydrophobic, superabsorbing materials from reduced graphene oxide/MoS_2 polyurethane foam as a promising sorbent for oil and organic solvents. Polym Test 87: e106429. http://doi.org/10.1016/j.polymertesting.2020.106429.

KARDEŞ M, DIZMAN B, ÖZTÜRK K & KÖSEOĞLU-İMER DY. 2025. ZnO Nanorod-Immobilized Polyurethane Foams for Efficient Removal of Gaseous Volatile Organic Compounds. ACS Appl Nano Mater 8: 7290-7303. https://doi.org/10.1021/acsanm.5c00665.

KNAPIK E & STOPA J. 2018. Fibrous deep-bed filtration for oil/water separation using sunflower pith as filter

media. Ecol Eng 121: 44-52. http://doi.org/10.1016/j.ecoleng.2017.07.021.

KO TJ, HWANG JH, DAVIS D, SHAWKAT MS, HAN SS, RODRIGUEZ KL, OH KH, LEE WH & JUNG Y. 2020. Superhydrophobic MoS_2-based multifunctional sponge for recovery and detection of spilled oil. Curr Appl Phys 20: 344-351. http://doi.org/10.1016/j.cap.2019.12.001.

LAGERGREN S. 1898. Zur theorie der sogenannten adsorption gelõster stoffe, Kungliga Svenska Vetenskapsakademiens. Handlingar 24: 1-39.

LEE J, PIAO L & PARK H. 2023. Characterization of the physical and weathering properties of low sulfur fuel oil (LSFO) and its spreading on water surface. J Hazard Mater 453: e131444. https://doi.org/10.1016/j.jhazmat.2023.131444.

LI B, LIU X, ZHANG X, ZOU J, CHAI W & LOU Y. 2015. Rapid adsorption for oil using superhydrophobic and superoleophilic polyurethane sponge. J Chem Technol Biotechnol 90: 2106-2112. http://doi.org/10.1002/jctb.4646.

LI H, LIU L & YANG F. 2012. Hydrophobic modification of polyurethane foam for oil spill cleanup. Mar Pollut Bull 64: 1648-1653. http://doi.org/10.1016/j.marpolbul.2012.05.039.

LI K, YU H, YAN J & LIAO J. 2020. Analysis of offshore oil spill pollution treatment technology. IOP Conference Series: Earth and Environmental Science 510: e042011. http://doi.org/10.1088/1755-1315/510/4/042011.

LI P, CAI Q, LIN W, CHEN B & ZHANG B. 2016. Offshore oil spill response practices and emerging challenges. Mar Pollut Bull 110: 6-27. http://doi.org/10.1016/j.marpolbul.2016.06.020.

LI WJ, SHI EW, ZHONG WZ & YIN ZW. 1999. Growth mechanism and growth habit of oxide crystal. J Cryst Growth 203: 186-196. https://doi.org/10.1016/S0022-0248(99)00076-7.

LU Y, WANG H & LU Y. 2019. An architectural exfoliated-graphene carbon aerogel with superhydrophobicity and efficient selectivity. Mater Des 184: e108134. https://doi.org/10.1016/j.matdes.2019.108134.

MAAMOUN AA, MAHMOUD AA, NAEIM DM, ARAFA M & ESAWI AMK. 2024. Effect of density and thickness of flexible polyurethane foam on the performance of triboelectric nanogenerators. Mater Adv 5: 6132-6144. https://doi.org/10.1039/d4ma00304g.

MAIA LS, NETO TS, PERLUXO JD, CARMO FL, ROSA DS & MULINARI DR. 2024. Eco-friendly sorbents for petroleum and diesel based on macadamia nutshell waste in castor oil-based polyurethane foam for oil spill. Adsorption 30: 2037-2051. https://doi.org/10.1007/s10450-024-00541-z.

MARTINS LS, ZANINI NC, MAIA LS, SOUZA AG, BARBOSA RFS, ROSA DS & MULINARI DR. 2021. Crude oil and S500 diesel removal from seawater by polyurethane composites reinforced with palm fiber residues. Chemosphere 267: e129288. https://doi.org/10.1016/j.chemosphere.2020.129288.

MIRANDA RJ, PINTO TKO, LOPES RVR, SANTOS JW, SAMPAIO CLS, SANTOS RG, PEREIRA PHC, CARDOSO ATC, MALHADO ACM & LADLE RJ. 2022. Oil spill disaster in southwest Atlantic coast: an evaluation of short-term effects on coral reef benthic assemblages. An Acad Bras Cienc 94: e20210401. https://doi.org/10.1590/0001-3765202220210401.

MOURA GB, SILVA AD, SALES EG, SOUZA RC, BRANCO JO & PASA EL. 2022. Solid waste management in a sustainable smart city in Brazil. Int J Sci Res 11: 822-830. https://www.ijsr.net/getabstract.php?paperid=SR221216143800.

MYINT MTZ, KUMAR NS, HORNYAK GL & DUTTA J. 2013. Hydrophobic/hydrophilic switching on zinc oxide micro-textured surface. Appl Surf Sci 264: 344-348. https://doi.org/10.1016/j.apsusc.2012.10.024.

NG ZC, ROSLAN RA, LAU WJ, GURSOY M, KARAMAN M, JULLOK N & ISMAIL AF. 2020. A green approach to modify surface properties of polyurethane foam for enhanced oil absorption. Polymers (Basel) 12: e1883. http://doi.org10.3390/polym12091883.

NOBRE P ET AL. 2022. The 2019 Northeast Brazil oil spill: scenarios. An Acad Bras Cienc 94: e20210391. https://doi.org/10.1590/0001-3765202220210391.

NWADIOGBU JO, AJIWE VIE & OKOYE PAC. 2016. Removal of crude oil from aqueous medium by sorption on hydrophobic corncobs: Equilibrium and kinetic studies. J Taibah Univ Sci 10: 56-63. http://doi.org/10.1016/j.jtusci.2015.03.014.

OLIVITO F, ALGIERI V, JIRITANO A, TALLARIDA MA, COSTANZO P, MAIUOLO L & NINO A. 2023. Bio-Based Polyurethane Foams for the Removal of Petroleum-Derived Pollutants: Sorption in Batch and in Continuous-Flow. Polymers 15: e1785. https://doi.org/10.3390/polym15071785.

ORABY H, HEGAZY GE, ELTALAWY SM & NABIL IM. 2025. Polyurethane-based foam composites: synthesis, structural characteristics, and radiation shielding properties. Sci Rep 15: 12227. https://doi.org/10.1038/s41598-025-95497-7.

PIAO L, PARK CJ, KIM S, PARK K, LEE Y, KIM HY, MOON MW & PARK H. 2023. Development of rapid and effective oil-spill response system integrated with oil collection, recovery and storage devices for small oil spills at initial stage: From lab-scale study to field-scale test. J Environ Manag 345: e118833. https://doi.org/10.1016/j.jenvman.2023.118833.

PINTO PCC, SILVA VR, YOSHIDA MI & OLIVEIRA MAL. 2018. Synthesis of flexible polyurethane foams by the partial substitution of polyol by steatite. Polímeros 28: 323-331. http://doi.org/10.1590/0104-1428.10417.

PIPEROPOULOS E, CALABRESE L, MASTRONARDO E, ABDUL-RAHIM SH, PROVERBIO E & MILONE C. 2018. Assessment of sorption kinetics of carbon nanotube-based composite foams for oil recovery application. J Appl Polym Sci 136: e47374. http://doi.org/10.1002/app.47374.

RAHMAN MM. 2020. Polyurethane/Zinc Oxide (PU/ZnO) Composite—Synthesis, Protective Property and Application. Polymers (Basel) 12: e1535. http://doi.org/10.3390/polym12071535.

ROCHA KR, CHIAVONE-FILHO O & OLIVEIRA HNM. 2023a. Post-Consumer Polyurethane Foams Hydrophobization Through Surface Modifications for Oil Spill Sorption. Mater Res 26: e20220536. http://doi.org/10.1590/1980-5373-mr-2022-0536.

ROCHA KR, CHIAVONE-FILHO O & OLIVEIRA HNM. 2023b. Influence of temperature on the recovery of oils spilled in seawater using hydrophobized post-consumer polyurethane foams. Braz J Petro Gas 17: 95-103. http://dx.doi.org/10.5419/bjpg2023-0006.

ROGINSKY SZ & ZELDOVICH J. 1934. An equation for the kinetics of activated adsorption. Acta Physicochim 1: 554-559. https://doi.org/10.1038/134935a0.

SANT'ANNA SS, SOUZA DA, ARAUJO DM, CARVALHO CF & YOSHIDA MI. 2008. Physico-chemical analysis of flexible polyurethane foams containing commercial calcium carbonate. Mater Res 11: 433-438. https://doi.org/10.1590/S1516-14392008000400009.

SCHUSTER P. 2019. What is special about autocatalysis? Monatsh Chem 150: 763-775. http://doi.org/10.1007/s00706-019-02437-z.

SEGOVIA M, LEMUS K, MORENO M, SANTA ANA MA, GONZALES G, BALLESTEROS B, SOTOMAYOR C & BENAVENTE E. 2011. Zinc oxide/carboxylic acid lamellar structures. Mater Res Bull 46: 2191-2195. http://doi.org/10.1016/j.materresbull.2011.06.040.

SILVA AVO & OLIVEIRA AKC. 2017. Análise dos parâmetros físico-químicos das águas da praia de Ponta Negra em Natal/RN – pH, turbidez, condutividade, salinidade e densidade. In: Proceedings of Congresso Internacional da Diversidade do Semiárido, 2., Campina Grande. Realize, p. 1-6. Available at: <https://editorarealize.com.br/artigo/visualizar/33124>. Acessed on Aug 2025.

SILVA IA, ALMEIDA FCG, SOUZA TC, BEZERRA KGO, DURVAL IJB, CONVERTI A & SARUBBO LA. 2022. Oil spills: impacts and perspectives of treatment technologies with focus on the use of green surfactants. Environ Monit Assess 194: e143. http://doi.org/10.1007/s10661-022-09813-z.

SOUZA LC & KOCK KDS. 2022. Análise do modelo logístico aplicado à primeira onda da Covid-19 nos países com os 20 maiores PIB'S. J Health Bio Sci 10: 1-7. http://doi.org/10.12662/2317-3076jhbs.v10i1.4226.p1-7.2022.

TOMON TRB, OMISOL CJM, AGUINID BJM, SABULBERO KXL, ALGUNO AC, MALALUAN RM & LUBGUBAN AA. 2024. A novel naturally superoleophilic coconut oil-based foam with inherent hydrophobic properties for oil and grease sorption. Sci Rep 14: e14223. https://doi.org/10.1038/s41598-024-64178-2.

TRINO LD, DIAS LFG, ALBANO LGS, BRONZE-UHLE ES, RANGEL EC, GRAEFF CFO & LISBOA-FILHO PN. 2018. Zinc oxide surface functionalization and related effects on corrosion resistance of titanium implants. Ceram Int 44: 4000-4008. http://doi.org/10.1016/j.ceramint.2017.11.195.

UDAYAKUMAR KV, GORE PM & KANDASUBRAMANIAN B. 2021. Foamed materials for oil-water separation. Chem Eng J Adv 5: e100076. https://doi.org/10.1016/j.ceja.2020.100076.

VESES A, SANAHUJA-PAREJO O, MARTÍNEZ I, CALLEN MS, LOPEZ JM, GARCIA T & MURILLO R. 2021. A pyrolysis process coupled to a catalytic cracking stage: A potential waste-to-energy solution for mattress foam waste. Waste Manag 120: 415-423. http://doi.org/10.1016/j.wasman.2020.09.052.

VOLIKOV AB, SOBOLEV NA, KHREPTUGOVA AN & PERMINOVA IV. 2023. Static and dynamic sorption of DOM on Bond Elute PPL and Bondesil PPL sorbents: physical-chemical characteristics. Sep Sci Technol 58: 642-653. http://doi.org/10.1080/01496395.2022.2145224.

WANG Y. 2023. What drives sustainable development? Evaluating the role of oil and coal resources for selected resource rich economies. Resour Policy 80: e103078. http://doi.org/10.1016/j.resourpol.2022.103078.

WEBER WJ & MORRIS JC. 1963. Kinetics of Adsorption on Carbon from Solution. J Sanit Eng Div 89: 31-59. http://doi.org/10.1061/JSEDAI.0000430.

WENZEL RN. 1936. Resistance of solid surfaces to wetting by water. Ind Eng Chem 28: 988-994. http://doi.org/10.1021/ie50320a024.

WU F, PICKETT K, PANCHAL A, LIU M & LVOV Y. 2019. Superhydrophobic polyurethane foam coated with polysiloxane-modified clay nanotubes for efficient and recyclable oil absorption. ACS Appl Mater Interfaces 11: 25445-25456. http://doi.org/10.1021/acsami.9b08023.

WU J, MA X, GNANASEKAR P, WANG F, ZHU J, YAN N & CHEN J. 2023. Superhydrophobic lignin-based multifunctional

polyurethane foam with SiO_2 nanoparticles for efficient oil adsorption and separation. Sci Total Environ 860: e160276. http://doi.org/10.1016/j.scitotenv.2022.160276.

YANEVA Z, KOUMANOVA B & GEORGIEVA N. 2012. Study of the mechanism of nitrophenols sorption on expanded perlite – equilibrium and kinetics modeling. Maced J Chem Chem Eng 31: 101-114. http://doi.org/10.20450/mjcce.2012.61.

ZAHRA M ET AL. 2022. Synthesis and characterization of polyurethane/zinc oxide nanocomposites with improved thermal and mechanical properties. Inorg Chem Commun 144: e109916. https://doi.org/10.1016/j.inoche.2022.109916.

ZARO M, SILVESTRE WP, FEDRIGO JG, ZENI M & BALDASSO C. 2021. Sorption of oils by a commercial non-woven polypropylene sorbent. Res Soc Dev 10: e554101422671. http://doi.org/10.33448/rsd-v10i14.22671.

ZHANG S, CHEN S, LI H, LAI X & ZENG X. 2022. Superhydrophobic, flame-retardant, and magnetic polyurethane sponge for oil-water separation. J Environ Chem Eng 10: e107580. http://doi.org/10.1016/j.jece.2022.107580.

ZIA KM, BHATTI IA, BARIKANI M, ZUBER M & SHEIKH MA. 2008. XRD studies of chitin-based polyurethane elastomers. Int J Biol Macromol 43: 136-141. http://doi.org/10.1016/j.ijbiomac.2008.04.009.

How to cite

ROCHA KR, CHIAVONE-FILHO O & OLIVEIRA HNM. 2025. Recycling and reuse of polyurethane mattresses for recovering oils spilled in seawater. An Acad Bras Cienc 97: e20250053. DOI 10.1590/0001-3765202520250053.

Manuscript received on January 14, 2025;
accepted for publication on June 27, 2025

KESLEI ROSENDO DA ROCHA[1]
https://orcid.org/0000-0002-6158-3786

OSVALDO CHIAVONE-FILHO[2]
https://orcid.org/0000-0002-1752-5757

HUMBERTO NEVES MAIA DE OLIVEIRA[3]
https://orcid.org/0000-0001-7465-9631

[1]Federal University of Rio Grande do Norte, Department of Postgraduate Studies in Chemical Engineering, Materials Technology Laboratory, Av. Senador Salgado Filho, 3000, Lagoa Nova, 59078-900 Natal, RN, Brazil

[2]Federal University of Rio Grande do Norte, Department of Postgraduate Studies in Chemical Engineering, Oil and Gas Teaching and Research Center - NUPEG I, Av. Senador Salgado Filho, 3000, Lagoa Nova, 59078-900 Natal, RN, Brazil

[3]Federal University of Rio Grande do Norte, Department of Postgraduate Studies in Chemical Engineering, Supercritical Technology and Biodiesel Laboratory, Av. Senador Salgado Filho, 3000, Lagoa Nova, 59078-900 Natal, RN, Brazil

Correspondence to: **Keslei Rosendo da Rocha**
E-mail: kesleirosendo@gmail.com

Author contributions

The conceptualization was elaborated by Keslei Rosendo da Rocha, Osvaldo Chiavone-Filho & Humberto Neves Maia de Oliveira. Literature review, experimental execution, data processing, and writing of the first version were carried out by Keslei Rosendo da Rocha. Osvaldo Chiavone-Filho & Humberto Neves Maia de Oliveira supervised the work and reviewed the final version of the paper.